Oil & Natural Gas Technology

DOE Award No.: DE-FE0000408

Quarterly Report
January 2011 – March 2011

Post Retort, Pre Hydro-treat Upgrading of Shale Oil

Submitted by:
Ceramatec Inc
2425 S. 900 W.
Salt Lake City, UT 84119

Prepared for:
United States Department of Energy
National Energy Technology Laboratory

April 29, 2011

Office of Fossil Energy

Table of Contents

LIST OF TABLES

LIST OF FIGURES

1. EXECUTIVE SUMMARY

In the 6th quarter considerable progress was made with regard to the reactor side and electrolysis side of the upgrading process. Sodium has been selected as the alkali metal to use for further development. Sulfur and nitrogen removal is best when sodium is utilized for all three oil stocks tested while the electrolysis of sodium sulfide is looking better than electrolysis of lithium. In the 6th quarter the electrolysis was performed repeatedly at a temperature above the melting point of sodium and the membranes have been holding up well. Upgrading with methane as the hydrogen donating gas provides nearly the same result has hydrogen in terms of sulfur, nitrogen, metals removal and API gravity increase. Expenditures to date are close to budget.

2. PROGRESS, RESULTS AND DISCUSSION

2.1 Task 1.0: Project Management Plan

The PMP was updated within 30 days and submitted to the Project Manager (Quarter 1).

2.2 Task 2.0: Upgrading Development

This task is related to developing the process of treating shale oil, or heavy oil at elevated temperature and pressure in the presence of an alkali metal, either sodium or lithium and also a hydrogen source, either hydrogen gas or methane (natural gas) to form an oil stream with reduced levels of sulfur, nitrogen and heavy metals and also in the process reducing the viscosity and increasing the API gravity. The object here is to determine the impact of various reaction parameters on product quality.

2.2.1 Sub task 2.1: Analytical Capability

Analytical Laboratory Set up

A LECO CHNS analyzer has been installed in our analytical laboratory and is currently being utilized to determine assays.

2.2.2 Sub-task 2.2: Upgrading Reactor and Separation Setup

Experimental

Several additional experiments were performed on upgrading of San Joaquin heavy crude oil (SJ), (Heavy Oil 1), Red Leaf shale oil (RL), (Shale Oil 1), and Oil Shale Exploration Company shale oil (OSEC), Shale Oil 2. All the experiments were performed with using Sodium or Lithium as the alkali metal, 180 gm (approx.) of oil as raw material, 1000 psig pressure (approx) and H2 or CH4 as hydrogen donating gas. Upon reaction, the product was subjected to centrifuging to separate the solid fraction (sulfides and possibly heavy metals) from liquid. Table 1 below shows the list of different experiments.

Table 1: List of Experiments Performed, CHNS Analysis, and Ratio of H, N, and S relative to C and the change of those ratios relative to the oil before treatment

Oil	Temp	Metal	H source	Charge	Chg/Theo	Min	C	H	N	S	H/C	N/C	S/C	ΔH/C	ΔN/C	ΔS/C
Heavy 1	375	Li	CH4	1.8	0.56	60	84.99	11.39	0.70	1.28	0.134	0.008	0.015	0.019	-0.071	-0.162
Heavy 1	375	Li	CH4	1.8	0.56	60	84.35	12.14	0.14	0.02	0.144	0.002	0.000	0.094	-0.813	-0.987
Heavy 1	375	Li	H2	1.8	0.56	60	85.38	11.32	0.72	1.30	0.133	0.008	0.015	0.008	-0.049	-0.153
Heavy 1	275	Li	H2	1.8	0.56	60	85.33	11.60	0.70	1.50	0.136	0.008	0.018	0.034	-0.075	-0.022
Heavy 1	375	Li	H2	1.9	0.59	120	84.75	11.63	0.69	1.29	0.137	0.008	0.015	0.044	-0.082	-0.153
Heavy 1	375	Li	H2	3.2	0.99	120	84.34	11.51	0.67	1.21	0.136	0.008	0.014	0.038	-0.104	-0.202
Heavy 1	375	Li	H2	3.2	0.99	120	84.72	11.08	0.70	1.23	0.131	0.008	0.015	-0.005	-0.068	-0.192
Heavy 1	375	Na	CH4	0.0	0.00	120	86.17	11.31	0.74	1.23	0.131	0.009	0.014	-0.002	-0.032	-0.206
Heavy 1	375	Na	CH4	6.0	0.56	60	83.79	11.25	0.67	1.07	0.134	0.008	0.013	0.021	-0.098	-0.289
Heavy 1	375	Na	CH4	6.0	0.56	60	16.27	10.97	0.13	0.13	0.674	0.008	0.008	4.127	-0.099	-0.555
Heavy 1	375	Na	CH4	10.6	0.99	120	86.91	12.53	0.10	0.03	0.144	0.001	0.000	0.096	-0.870	-0.981
Heavy 1	375	Na	H2	0.0	0.00	60	85.70	11.46	0.71	1.36	0.134	0.008	0.016	0.017	-0.066	-0.117
Heavy 1	375	Na	H2	0.0	0.00	120	86.20	11.20	0.73	1.23	0.130	0.008	0.014	-0.012	-0.045	-0.206
Heavy 1	375	Na	H2	6.0	0.56	60	85.56	11.72	0.68	0.27	0.137	0.008	0.003	0.042	-0.104	-0.824
Heavy 1	375	Na	H2	10.3	0.96	120	86.18	12.50	0.19	0.04	0.145	0.002	0.000	0.103	-0.751	-0.974
Heavy 1	375	Na	H2	10.7	1.00	120	86.51	12.20	0.13	0.02	0.141	0.002	0.000	0.072	-0.831	-0.987
Heavy 1	375	Na	H2	10.7	1.00	120	15.00	11.33	0.03	0.01	0.755	0.002	0.001	4.744	-0.774	-0.963
Heavy 1	250	Na	H2	10.7	1.00	120	85.31	11.14	0.74	1.42	0.131	0.009	0.017	-0.007	-0.022	-0.074
Heavy 1	375	Na	H2	6.0	0.56	30	85.61	11.51	0.77	0.37	0.134	0.009	0.004	0.022	0.014	-0.759
Oil	Temp	Metal	H source	Charge	Chg/Theo	Min	C	H	N	S	H/C	N/C	S/C	ΔH/C	ΔN/C	ΔS/C
Shale 1	375	Li	CH4	1.8	0.43	60	85.59	12.40	1.29	0.17	0.145	0.015	0.002	-0.007	-0.140	-0.329
Shale 1	375	Li	H2	0.9	0.22	60	85.71	12.28	1.35	0.22	0.143	0.016	0.003	-0.018	-0.101	-0.133
Shale 1	375	Li	H2	1.8	0.43	60	85.15	12.49	1.23	0.10	0.147	0.014	0.001	0.005	-0.175	-0.603
Shale 1	275	Li	H2	1.8	0.43	60	84.88	12.33	1.35	0.18	0.145	0.016	0.002	-0.005	-0.092	-0.283
Shale 1	375	Li	H2	4.2	1.01	120	85.81	12.92	0.13	0.01	0.151	0.002	0.000	0.032	-0.914	-0.961
Shale 1	250	Li	H2	4.2	1.01	120	84.84	12.14	1.34	0.20	0.143	0.016	0.002	-0.020	-0.098	-0.203
Shale 1	150	Na	CH4	6.0	0.44	60	85.04	12.83	0.68	0.15	0.151	0.008	0.002	0.034	-0.544	-0.404
Shale 1	375	Na	CH4	6.0	0.44	60	85.72	12.51	0.71	0.06	0.146	0.008	0.001	0.000	-0.527	-0.763
Shale 1	375	Na	CH4	13.7	0.99	120	86.15	13.62	0.04	0.03	0.158	0.000	0.000	0.083	-0.973	-0.882
Shale 1	375	Na	H2	0.0	0.00	60	85.69	12.29	1.33	0.25	0.143	0.016	0.003	-0.017	-0.114	-0.014
Shale 1	375	Na	H2	1.6	0.11	60	85.55	12.21	1.27	0.19	0.143	0.015	0.002	-0.022	-0.153	-0.250
Shale 1	375	Na	H2	3.0	0.22	60	84.88	12.30	1.29	0.11	0.145	0.015	0.001	-0.007	-0.132	-0.562
Shale 1	375	Na	H2	5.9	0.43	30	85.79	12.33	1.48	0.25	0.144	0.017	0.003	-0.015	-0.015	-0.015
Shale 1	375	Na	H2	6.0	0.44	60	85.86	13.05	0.64	0.03	0.152	0.007	0.000	0.041	-0.575	-0.882
Shale 1	375	Na	H2	13.7	0.99	120	86.06	13.55	0.03	0.01	0.157	0.000	0.000	0.079	-0.980	-0.961
Shale 1	375	Na	H2	13.7	0.99	120	85.69	12.98	0.30	0.02	0.151	0.004	0.000	0.038	-0.800	-0.921
Shale 1	250	Na	H2	13.7	0.99	120	84.76	12.82	0.80	0.04	0.151	0.009	0.000	0.036	-0.461	-0.841
Oil	Temp	Metal	H source	Charge	Chg/Theo	Min	C	H	N	S	H/C	N/C	S/C	ΔH/C	ΔN/C	ΔS/C
Shale 2	375	Li	CH4	1.9	1.11	120	86.12	12.76	0.35	0.34	0.148	0.004	0.004	-0.002	-0.164	-0.573
Shale 2	375	Li	H2	1.8	1.06	60	85.36	12.69	0.38	0.40	0.149	0.004	0.005	0.001	-0.084	-0.493
Shale 2	275	Li	H2	1.8	1.06	60	84.59	12.62	0.40	0.66	0.149	0.005	0.008	0.005	-0.027	-0.156
Shale 2	375	Li	H2	1.8	1.06		86.04	12.92	0.33	0.37	0.150	0.004	0.004	0.011	-0.211	-0.535
Shale 2	375	Li	H2	1.9	1.11	120	86.06	13.08	0.37	0.39	0.152	0.004	0.005	0.024	-0.115	-0.510
Shale 2	250	Li	H2	1.9	1.11	120	85.25	12.65	0.42	0.65	0.148	0.005	0.008	-0.001	0.014	-0.175
Shale 2	375	Li	H2	6.0	3.52	60	80.10	11.64	0.21	0.76	0.145	0.003	0.009	-0.021	-0.460	0.026
Shale 2	375	Na	CH4	6.0	1.06	60	85.95	13.06	0.25	0.03	0.152	0.003	0.000	0.023	-0.401	-0.962
Shale 2	375	Na	CH4	6.3	1.12	120	86.37	12.96	0.24	0.03	0.150	0.003	0.000	0.010	-0.428	-0.962
Shale 2	375	Na	H2	0.0	0.00	60	85.38	12.77	0.39	0.77	0.150	0.005	0.009	0.007	-0.060	-0.024
Shale 2	375	Na	H2	1.5	0.27	60	85.33	12.81	0.40	0.62	0.150	0.005	0.007	0.011	-0.035	-0.214
Shale 2	375	Na	H2	3.0	0.53	60	85.77	12.99	0.39	0.51	0.151	0.005	0.006	0.020	-0.064	-0.357
Shale 2	375	Na	H2	6.0	1.06	60	86.41	13.36	0.16	0.02	0.155	0.002	0.000	0.041	-0.619	-0.975
Shale 2	375	Na	H2	6.3	1.12	120	86.37	13.53	0.18	0.03	0.157	0.002	0.000	0.055	-0.571	-0.962
Shale 2	375	Na	H2	6.3	1.12	120	86.34	13.16	0.24	0.12	0.152	0.003	0.001	0.026	-0.428	-0.850
Shale 2	250	Na	H2	6.3	1.12	120	84.62	13.00	0.25	0.07	0.154	0.003	0.001	0.035	-0.392	-0.911

2.3 Results and Discussions

2.3.1 CHNS

The data was analyzed in several different ways to determine which variable had the most impact and to determine under what conditions. For the case of Heavy Oil 1, two runs highlighted in the table had C analyses which appeared incorrect so the results were not included in the analysis.
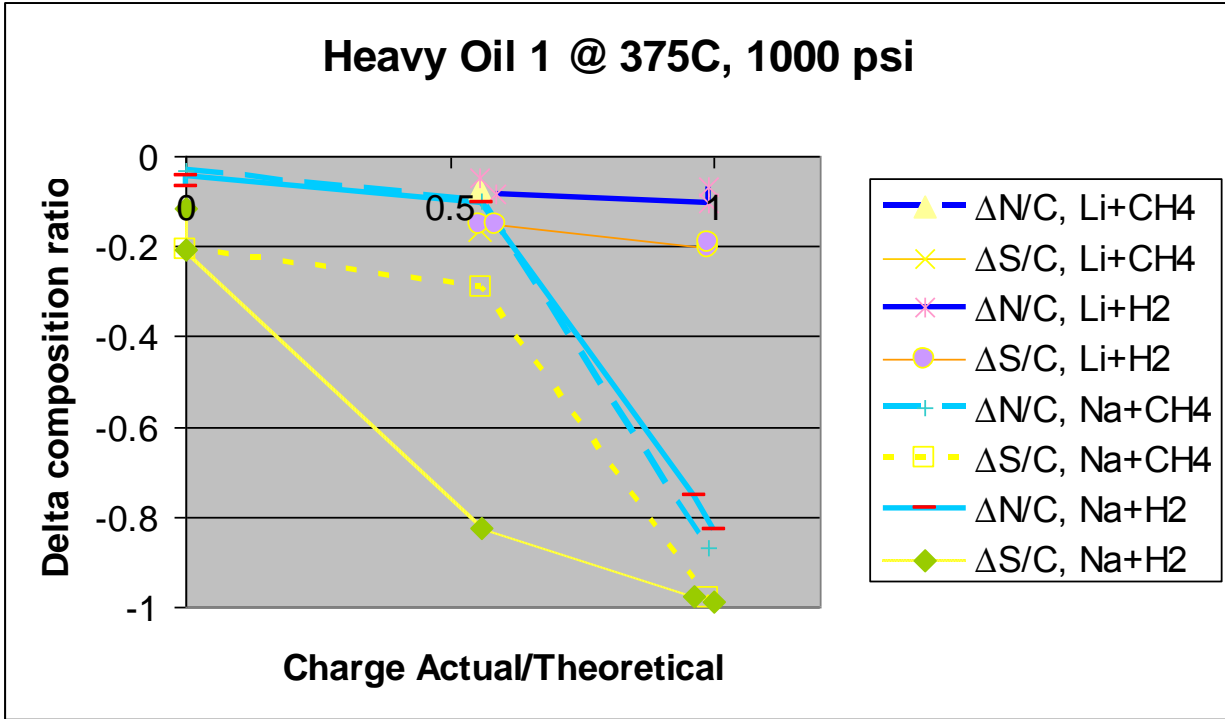
Figure 1: Heavy Oil 1 Change in Composition versus Charge Actual/Theoretical

       Figure 1 shows a plot of the change in N/C and S/C ratios for Heavy Oil 1 as the Na or Li charge Actual/Theoretical charge varies from 0 to approximately 1 and where either CH4 or H2 gas was the hydrogen donor. We can see that the change in composition ratio is much greater when Na is used versus Li. We also see that the sulfur ratio changes more readily than nitrogen, especially when the Actual/Theoretical charge is less than 1. We also see that when the Actual/Theoretical charge approaches 1, there is little difference between utilization of hydrogen or CH4 has the hydrogen donor.
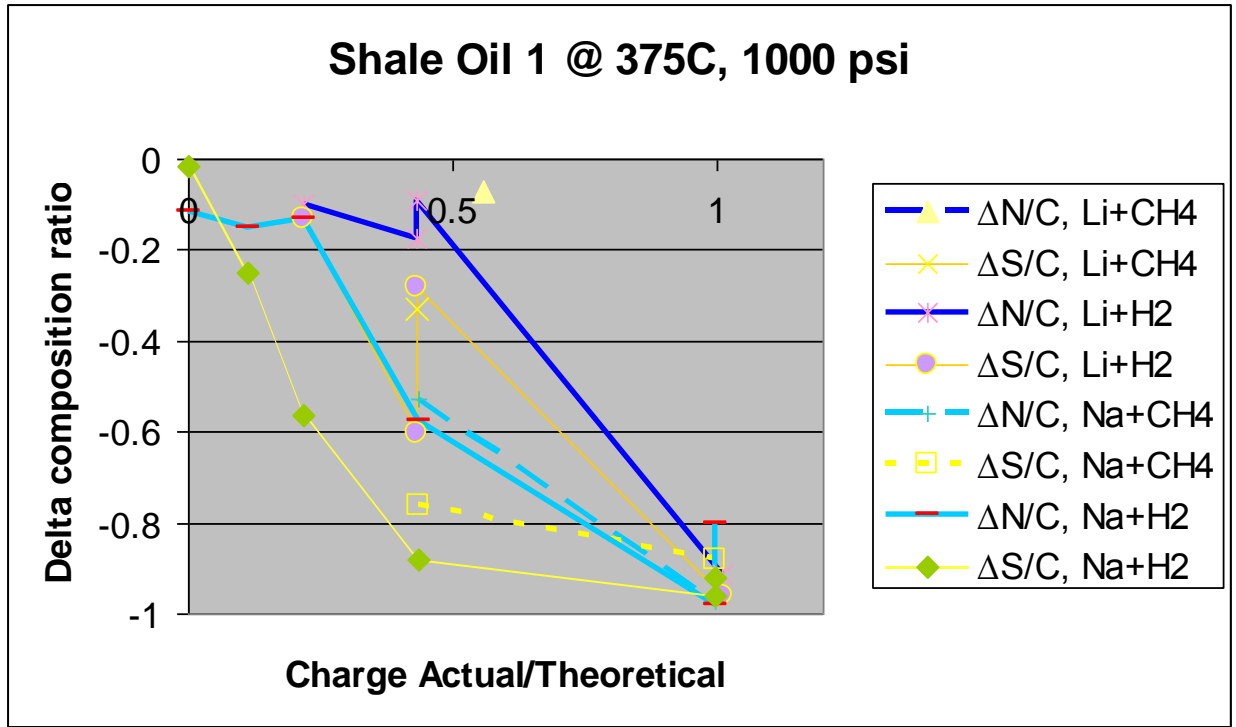
Figure 2: Shale Oil 1 Change in Composition versus Charge Actual/Theoretical

Figure 2 shows a plot of the change in N/C and S/C ratios for Shale Oil 1 as the Na or Li charge Actual/Theoretical charge varies from 0 to approximately 1 and where either CH4 or H2 gas was the hydrogen donor. We can see that the change in composition ratio is much greater when Na is used versus Li at low Actual/Theoretical but not at high.. We also see that the sulfur ratio changes more readily than nitrogen, especially when the Actual/Theoretical charge is less than 1. We also see that when the Actual/Theoretical charge approaches 1, there is little differ-ence between utilization of hydrogen or CH4 has the hydrogen donor.
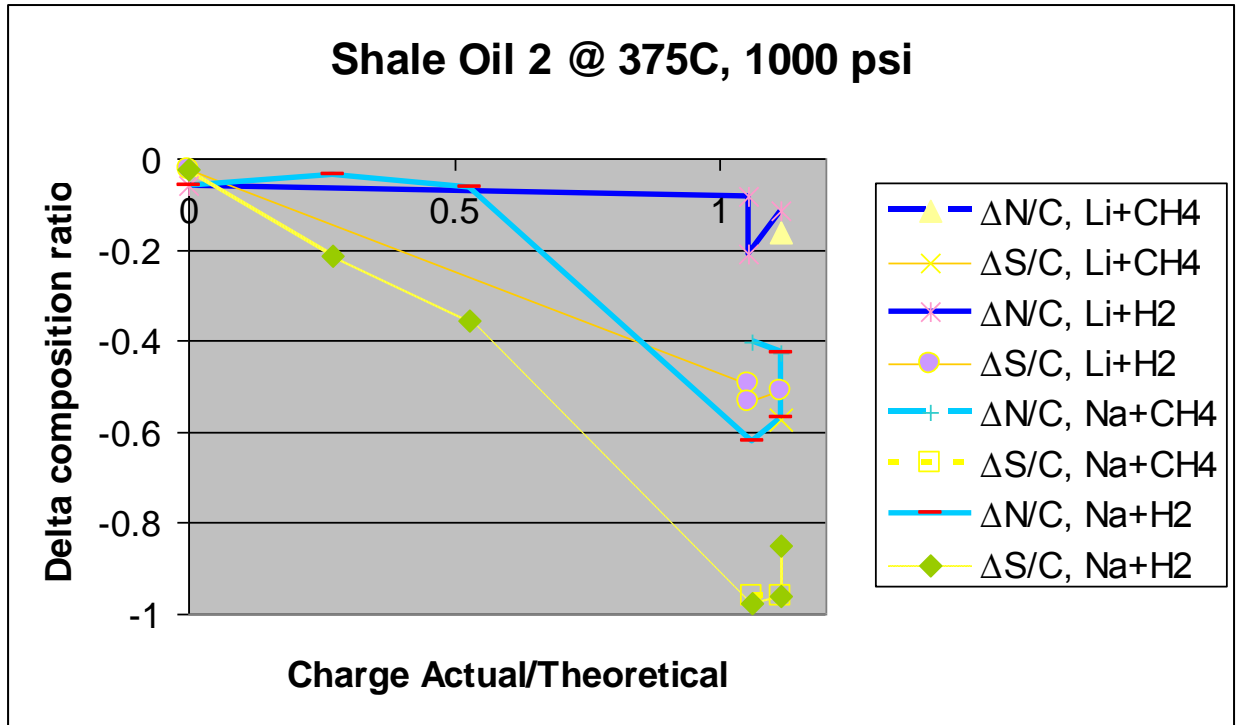
Figure 3: Shale Oil 2 Change in Composition versus Charge Actual/Theoretical

Figure 3 shows a plot of the change in N/C and S/C ratios for Shale Oil 2 as the Na or Li charge Actual/Theoretical charge varies from 0 to approximately 1 and where either CH4 or H2 gas was the hydrogen donor. We can see that the change in composition ratio is much greater when Na is used versus Li. We also see that the sulfur ratio changes more readily than nitrogen, especially when the Actual/Theoretical charge is less than 1. There is little data to compare H2 versus CH4 in this data set.

2.3.2 Inductive Coupled Plasma (ICP)

Inductive coupled plasma measurements were performed for all three feedstocks .Table 2 below shows the results of ICP measurements on feedstocks and Table 3 below shows the measurements of products in Heavy Oil and their conversion with Sodium and either hydrogen or methane.

Table 2: ICP measurements on different feedstocks

Element/Feed	Fe	Al	Cr	Cu	Mo	Si	V	Zn	Ni	Hg	As	Co
RL	36.54	9.533	0	0.181	0	2.544	0.293	8.199	0.756	0	29.01	0
OSEC	0[1]	9.99	0	0	0	104	0.353	0.541	0	0	0	0
SJ	218	55.35	0	0	0	3.476	197	9.47	331.4	0	0	0

---

[1] 0 is undetectable.

Table 3: ICP measurement of products in Heavy Oil and Conversion with Sodium and either hydrogen or methane

	Heavy Oil with H_2 & Na			Heavy Oil with CH_4 & Na		
	In	Out	Convers.	In	Out	Convers.
Fe ppm	218.0	0	100%	218	2.39	99%
V ppm	197.0	0	100%	197	1.31	99%
Ni ppm	331.4	0	100%	331.4	0.85	100%

Schedule

The progress of Task 2 is as per schedule.

2.4   Task 3.0 – Electrolysis Development

To reduce the overall cost of the upgrading process, an electrolysis process will be developed to regenerate sodium or lithium from the respective polysulfide. The process will feature ceramic ion conductive membranes developed at Ceramatec. The energy cost to regenerate the alkali metals from the polysulfide is expected to be about half that of producing the metals from their respective chlorides.

2.4.1   Subtask 3.1 – Membrane fabrication

The Recipient shall fabricate and characterize sodium conductive and lithium conductive membranes.

Ionic Conductivity Measurement of LiSICON 10B

The ionic conductivity of LiSICON 10B has been measured by AC Impedance Spectroscopy within the temperature range from ambient to 150ºC (Figure 4). Both bulk and boundary grain contributions to the total ionic conductivity of the material are included in the reported data. For comparison purposes, the latest NaSICON-GY data available (from 2008) has been added to the graph. It can be seen that LiSICON 10B is approximately two times more conductive than NaSICON-GY at 150ºC. These results are very encouraging and add to the improvements achieved in the strength of the material, which were reported in the previous quarterly report.
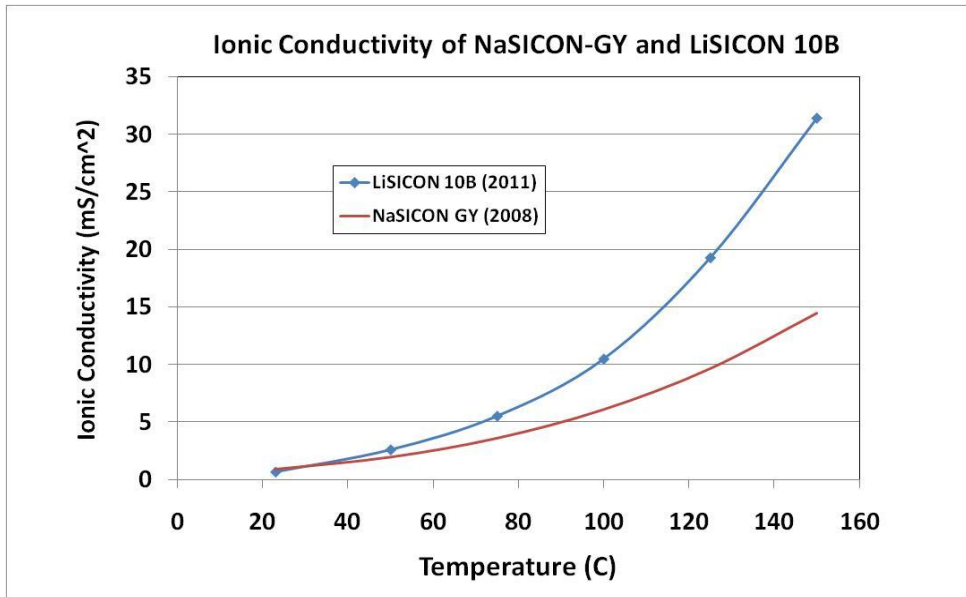
Figure 4: Ionic conductivity of LiSICON 10B versus temperature and comparison with NaSICON-GY

2.4.2 Subtask 3.2 – Seal testing

Ceramatec shall evaluate various seal approaches for compatibility with the alkali metal and the metal polysulfide at various temperatures.

Successfully tested a silica-boria glass material to bind 1" OD alumina tubes to 1" diameter (0.5 to 1.0 mm thick) NaSICON disks. This is the approach used to seal the cathode side (inside tube) from the anode side (outside tube) in molten sodium recovery cells (see Figure 5). The glass powder material requires a firing temperature of 850°C for 15 minutes to fully densify. 100% yield of leak tight seals was achieved with the 1 mm thick membranes, whereas 75% yield was obtained with the 0.5 mm thick membranes. The yield difference is explained by the better flatness spec of the thicker membranes. The high temperature and corrosion resistant properties of the material has met all our expectations. Molten sodium recovery test cells, using this type of glass seals, have been in operation for over 300 hours at temperatures up to 160ºC without failure.

Figure 5: Anode side [A] and cathode side [B] of a Molten Sodium Recovery Cell showing the glass seal

2.4.3   Subtask 3.3 – Cell design and set up

Ceramatec shall design benchtop cells for two types of operation, one where the alkali metal is molten and one where it plates onto a current collector. Reactors and catholyte transfer means will be provided to prepare alkali metal sulfide of differing composition and transfer to the cell. The cells will be designed to accommodate multiple reference electrodes, operate at various elevated temperatures. The cells will have features designed to facilitate sulfur removal and be designed to operate within a dry enclosure.

Electrolysis Test Cell Design

A 500 ml flask with a 300W built-in heater (Ace Glass Instatherm Flask) has been acquired during this quarter. The new glass flask has replaced the heating plate used to run the molten sodium recovery cells in the past. In addition, a feedback temperature controller with ±0.1°C control accuracy and ramping capabilities is now used to control the cell's temperature. This lab equipment addition has resulted in a much tighter control of the cell's operating temperature and in a significant reduction of the waste heat released inside the glove box.

2.4.4   Subtask 3.4 – Cell operation

The Recipient shall operate cells under various conditions including variation of the current density, electrode gap, temperature, electrolyte, polysulfide order, and alkali metal. Current will be measured as a function of applied voltage. Periodically cell operation will be interrupted and cell contents analyzed to determine current efficiency. In Phase 1 the alkali metal polysulfide will be synthesized from alkali metal and sulfur and will not contain appreciable impurities which may flow through from an actual upgrading process as will occur in Phase 2.

Molten Sodium Recovery Test Cell Runs Results
A total of 5 molten sodium recovery test cells have been assembled and run during this reporting period.

Table 4 summarizes the test cells construction properties and the runs operating conditions. All the cells were built using the new silica-boria glass seal. This has allowed us to conduct long term cell performance testing, up to temperatures of 160ºC, without seeing any seal failures up to date. The main focus of the testing, in this quarter, has been in studying the performance of the NaSICON membranes during hundreds of hours of continuous operation. The cells were operated within a temperature range of 130 to 160ºC and at current densities from 25 to 150 mA/cm^2. NaSICON-GY disks of 0.5 mm and 1 mm thickness were used.

The main conclusions learnt from these runs are summarized below.

1. Long term operation of molten sodium/NaSICON/Na$_2$S$_4$ recovery cells for hundreds of hours have been accomplished in this quarter. Figure 6, Figure 7, and Figure 8 show plots of cell voltage and current density for the three longest running cells tested in this period. During cell operation, sodium polysulfide (Na$_2$S$_4$) is periodically added to the anolyte solution to replenish the sodium separated. Sodium metal is also periodically removed as it accumulates inside the alumina tube of the cell. Table 5 reports total cell run time, total sodium polysulfide added, total sodium recovered, and the condition of the membranes by the end of the test. Cell voltage is affected by many parameters such as sodium ion concentration, temperature, current density, electrolyte ionic conductivity and others. The voltage profiles shown in the figures reflect changes in these parameters that occurred during the run tests.

2. We have observed that the tested NaSICON membranes developed an increasing and irreversible over potential, which seemed to correlate with the gradual darkening of the membrane's anode active surface (Figure 10 [A]). It is believed that corrosion, caused by the polysulfides, is responsible for the color change in the surface. This corrosion eventually led to the failure of the membrane in cell Na_molten_20110202, as shown in Figure 10 [A] and [B]. The failure occurred after 270 hours of operation. A somewhat different failure mechanism was responsible for ending cell Na_molten_20110117 after 198 hours of operation. In this case, multiple cracks can be observed throughout on both sides of the membrane (Figure 11 [A] and [B]). More experimental data will be needed to fully understand the corrosion process so as to assess the life expectancy of the NaSICON-GY membranes under the demanding cell operating conditions.

3. Cell *Na_molten_20110311* has logged 366 hours so far and it is still in operation. The cell is running at 140ºC and 50-100 mA/cm^2. The main difference is that a much tighter temperature control (±0.1ºC) has been implemented, as compared to previous cells where temperature fluctuated as much as ±5ºC during operation. Whether tighter temperature control plays a role in the life expectancy of the membrane or not still needs to be proven.

4. Figure 9 displays the Open Circuit Voltage (OCV) profile for cell *Na_molten_20110311* through the run. The cell OCV is a function of temperature, sodium and polysulfide ions concentration, and the type of polysulfide ions in solution. At the beginning of the run, the OCV value was equal to 1.85V and it slowly increases as the sodium ions get depleted from the anolyte. Every time more sodium polysulfide (Na$_2$S$_4$) is added to the anolyte (batch feeds), then the OCV drops due to the increased concentration of Na$^+$ ions. In addition, higher order polysulfide ions (longer chain of sulfur atoms) have smaller oxidation potentials than lower order polysulfides. Therefore, the cell OCV also increases due to the progressive enrichment of the anolyte solution in higher order polysulfides as the

run goes on. As a result, the OCVs varied within the range 2.15-2.28V during the latest Na_2S_4 addition/Na depletion cycle.

5. Through all the test cell runs, we have not detected elemental sulfur precipitating out of the anolyte solution. In view of this fact, our hypothesis that elemental sulfur would eventually form as result of the oxidation of the S_8^{-2} polysulfide ion might be proven wrong. Recently, we have found some evidence in the literature that much longer chain polysulfide ions can form and be stable in solution. We are currently implementing an analytical method to quantify the S to Na ratio in the anolyte solution. Once this method is available, we will be able to characterize the average order of the polysulfide blend present in the anolyte solution and reported it as a function of cell run time.

Table 4: Sodium recovery test cells assembled and tested during the reporting period

Cell ID#	Anolyte	Anode Electrode	Membrane	Catholyte	Cathode Electrode	Seal Type	Operating Conditions
Na_molten_20110106	0.7 M Na2S4 in MF	Platinized Ti mesh (1.1" diam.)	NaSICON GY (1 mm thick, 0.8" diam.)	Molten Na	Molten Na, Ti rod current collector	Silica-Boria Glass	Temperature=130C Anolyte agitation Cte DC voltage=5 V
Na_molten_20110117	0.7 M Na2S4 in MF	Platinized Ti mesh (1.1" diam.)	NaSICON GY (1 mm thick, 0.8" diam.)	Molten Na	Molten Na, Ti rod current collector	Silica-Boria Glass	Temperature=130-150C Anolyte agitation Cte Voltage=4-5V Cte Current=35-125 mA/cm^2
Na_molten_20110128	0.7 M Na2S4 in MF	Platinized Ti mesh (1.1" diam.)	NaSICON GY (0.5 mm thick, 0.8" diam.)	Molten Na	Molten Na, Ti rod current collector	Silica-Boria Glass	Temperature=150-155C Anolyte agitation Cte Current=100 mA/cm^2
Na_molten_20110202	0.7 M Na2S4 in MF	Platinized Ti mesh (1.1" diam.)	NaSICON GY (0.5 mm thick, 0.8" diam.)	Molten Na	Molten Na, Ti rod current collector	Silica-Boria Glass	Temperature=135-150C Anolyte agitation Cte Voltage=5V Cte Current=35-150 mA/cm^2
Na_molten_20110311	0.7 M Na2S4 in MF	Platinized Ti mesh (1.1" diam.)	NaSICON GY (0.5 mm thick, 0.8" diam.)	Molten Na	Molten Na, Ti rod current collector	Silica-Boria Glass	Temperature=140-160C Anolyte agitation Cte Current=50-150 mA/cm^2

Table 5: Summary of sodium recovery test cell run results

Cell ID	Membrane ID	Total Run Time	Na2S4 Added	Na Recovered		Notes
		hours	grams	grams	% out of amount added	
Na_Molten_20110106	NAS-GY-58	25	36.5	7.42	76.90%	Accidentally broke membrane during cleaning
Na_Molten_20110117	NAS-GY-70	198	228.5	36.06	59.69%	Membrane failed during test.
Na_Molten_20110128	NAS-GY-65	6.2	49.1	1.33	10.25%	Membrane still in good condition
Na_Molten_20110202	NAS-GY-63	270	214.8	44.09	77.64%	Membrane failed during test.
Na_Molten_20110311	NAS-GY-68	368.4	360.89	51.35	53.82%	Cell still running
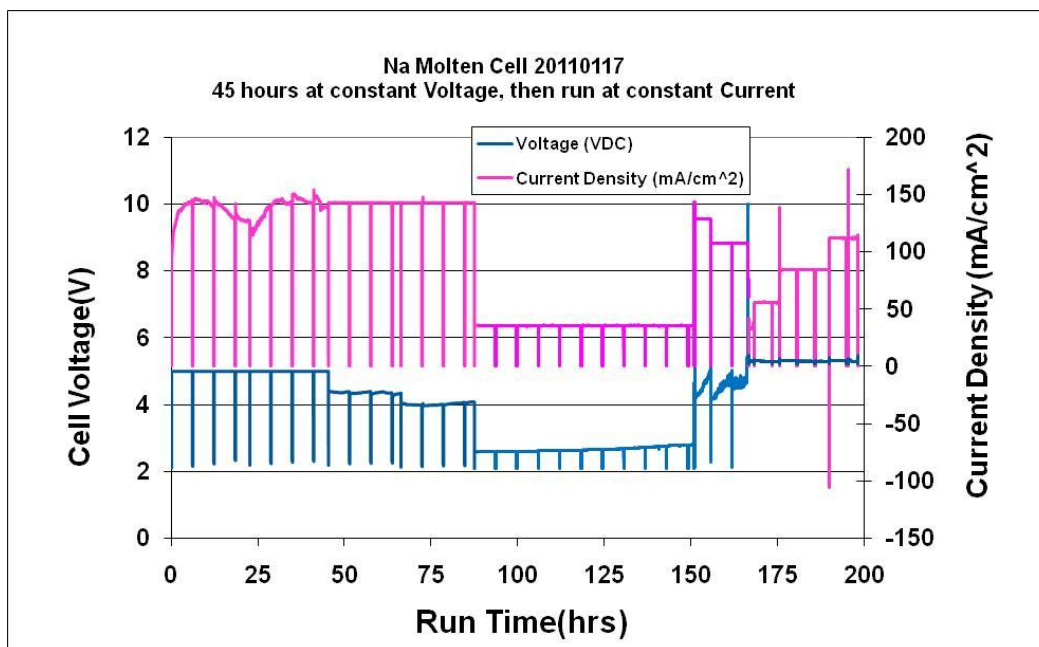
Figure 6: Current density and cell voltage for sodium recovery cell *Na_molten_20110117*. The Open Circuit Voltage (OCV) was measured every six hours of continuous operation
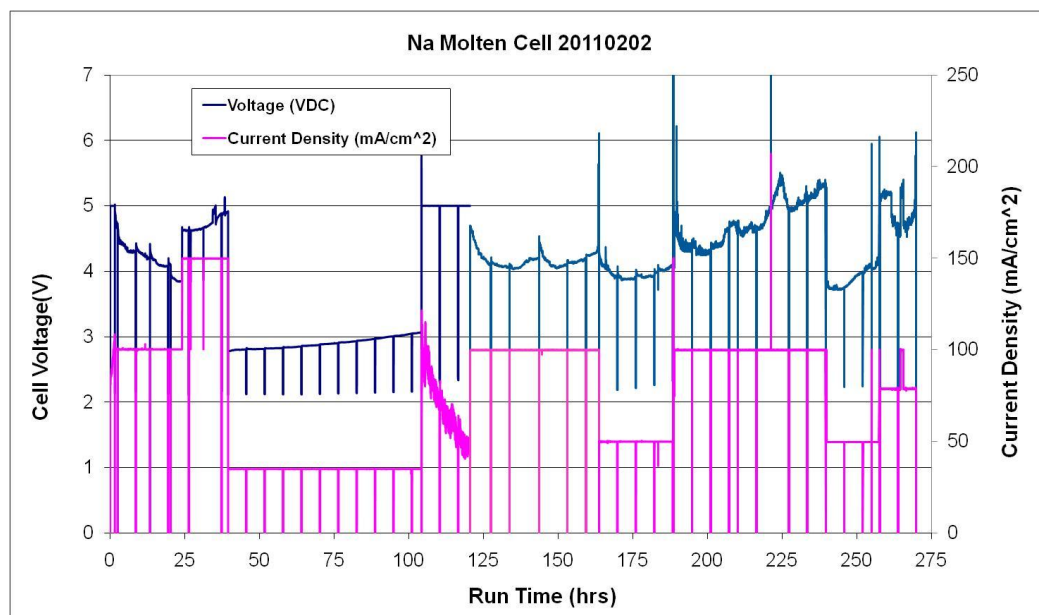
Figure 7: Current density and cell voltage for sodium recovery cell *Na_molten_20110202*. The Open Circuit Voltage (OCV) was measured every six hours of continuous operation
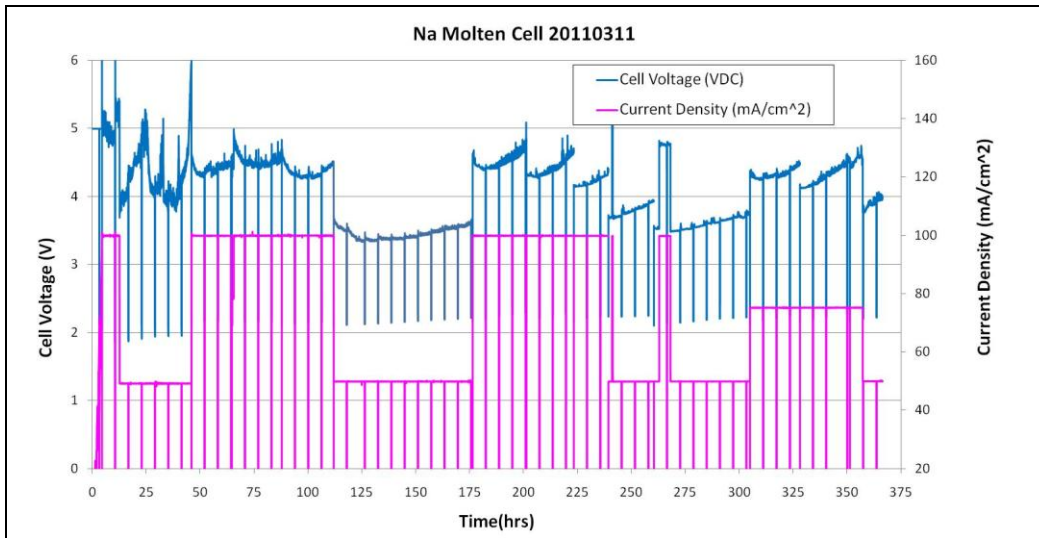
Figure 8: Current density and cell voltage for sodium recovery cell *Na_molten_20110311*. The Open Circuit Voltage (OCV) was measured every six hours of continuous operation
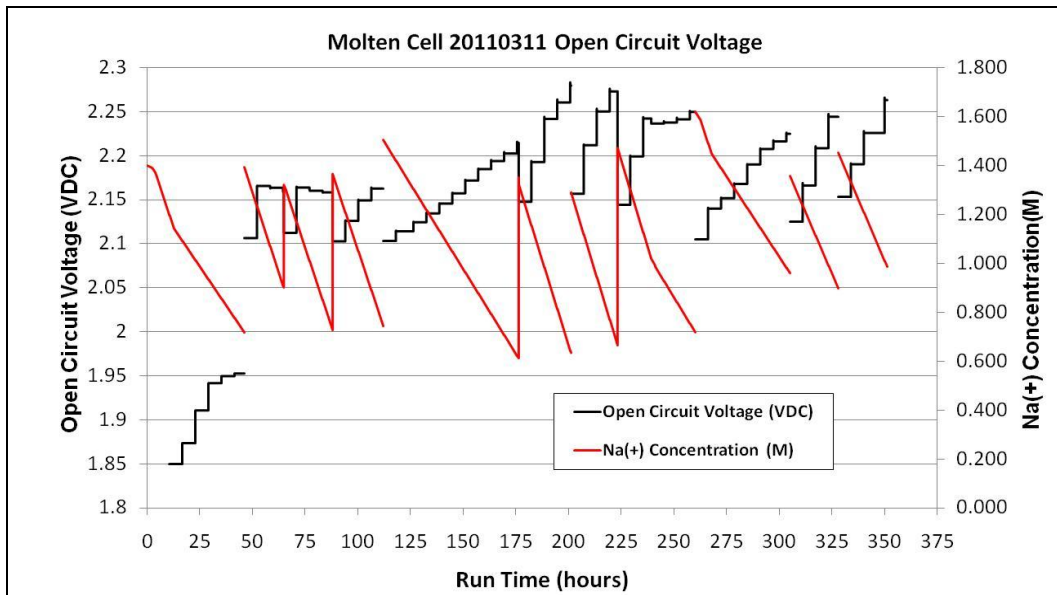
Figure 9: Cell Open Circuit Voltage (OCV) and sodium ion concentration for sodium recovery cell *Na_molten_20110311*

Figure 10: Anode [A] and cathode [B] sides of cell *Na_molten_20110202* at the end of the run after 270 hours of operation
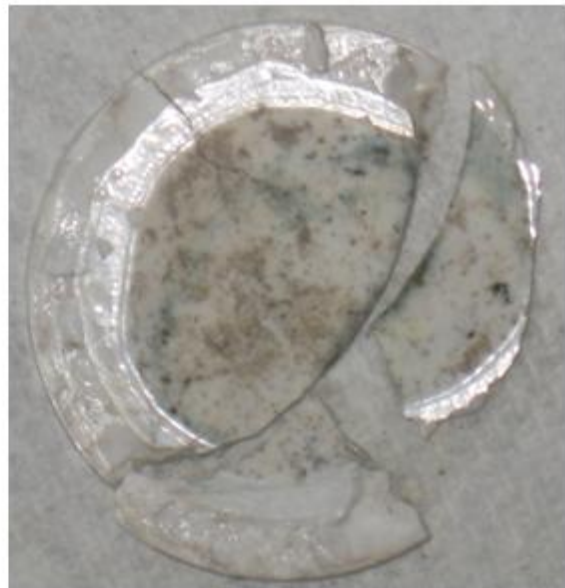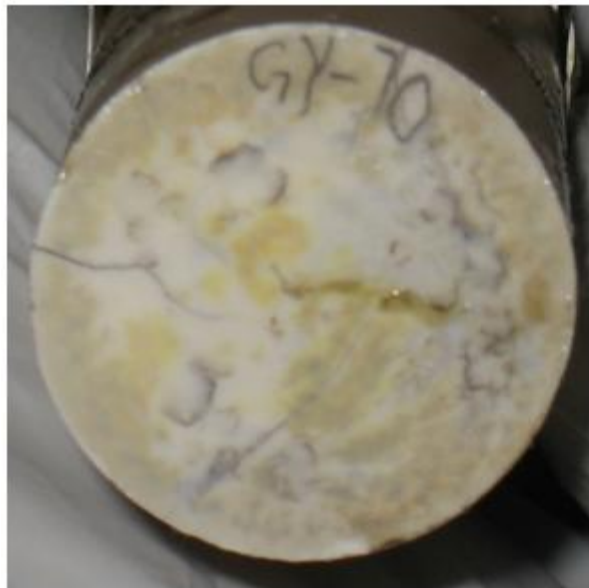
Figure 11: Anode [A] and cathode [B] sides of cell *Na_molten_20110117* at the end of the run after 198 hours of operation

Lithium Recovery Test Cell Runs

A total of three lithium recovery cells were assembled and run in this period. All the tests were conducted using the Dual Flow Test Cells in continuous closed-loop flow mode. Table 6 summarizes the cell construction properties and the runs operating conditions. The first two runs

of the set were done at ambient temperature, whereas the last test was done at 50ºC. As opposed to previous runs, where the cell was kept inside a temperature controlled oven, the cell's temperature was maintained by heating and flowing through the cell the anolyte and catholyte solutions. Due to the fact that the Dual Flow Test Cells are not designed to remove lithium metal from the cathode during operation, the cells had to be stopped and disassembled approximately every 24 hours of operation so they could be cleaned out. The main conclusions learnt from these runs are summarized below.

1. Long term discontinuous operation of a lithium recovery cell, fitted with a LiSICON 10B membrane has been demonstrated. Test cell *Li Recovery Dual Flow 20110111* logged 260 hours of operation at ambient temperature before the test was ended to free the lab equipment for new runs. During the experiment, a total of 1037 mg of lithium metal were recovered from the anolyte (Figure 15). Figure 12 shows the measured cell current density versus elapsed time at constant voltage (6 VDC) for the entire run. The average current density was close to 1 mA/cm^2 with peaks of up to 5 mA/cm^2. These short lasting current peaks occurred when cell power was resumed after each of the scheduled current interruption periods to measure the Open Circuit Voltage (OCV). A look over a shorter time span (Figure 13) reveals that the current fluctuated cyclically around the average value. This was most likely due to the effect of the controllers on the electrolytes temperature, which in turn maintained the cell's temperature.

2. Temperature has a significant effect on the ionic conductivity of the membrane and the electrolytes and therefore on the overall cell resistance. The current density was increased by almost an order of magnitude when the cell was operated at 50ºC, as compared to ambient temperature. Figure 14 illustrates this effect, showing the current density data of cell *Li Recovery Dual Flow 20110111* during a one day run. The current density remained around 8-10 mA/cm^2, for the first ten hours of the run, until it slowly dropped to 3.5 mA/cm^2 twenty hours into the run. This current density drop is probably explained by the increase of the cathode electrode resistance as the porous deposit of lithium metal accumulated on the electrode.

3. All the data collected, up to date, seems to indicate that LiSICON 10B material is very reliable for this application. Several membranes have run for a time in excess of 100 hours, without any measurable performance issues. We have observed that when lithium metal contacts the membrane surface during cell operation, a permanent black stain is formed on the membrane. This happens, for instance, when lithium particles break free from the cathode electrode surface and fall onto the membrane. Figure 16[A] and Figure 17[A] show pictures of the cathode side of the membrane from cell *Li Recovery Dual Flow 20110111* taken after 28 hours and 260 hours of run time, respectively. Obviously, this can be easily avoided by a cell design that removes lithium metal continuously. The appearance of an intense blue coloration on the anode side of the LiSICON 10B membranes have been described in previous quarterly reports. Figure 16[B] and Figure 17[B] demonstrate that although this phenomenon initiates as soon as power is applied to the cell, the area covered and the intensity of the color has not changed after 260 hours of operation.

4. Varying the catholyte and anolyte flow rates had not measurable effect on the cell's operating current density. This indicates that, even at 50°C operating temperature, the cell reactions are not mass transfer controlled.

Table 6: Lithium recovery test cells assembled and tested during the reporting period

Cell ID#	Anolyte	Anode Electrode	Membrane	Catholyte	Cathode Electrode	Operating Conditions
Li_Recovery_Dual_Flow_Cell 20110105	0.2 M Li2S in MF	Glassy carbon plate (1.65"x1.75", 0.5 mm thick) 3 mm to membrane	LiSICON 10B 1.5" Diam., 1 mm thick	1M LiI in TG	Titanium mesh (1.65"x1.75", 0.2 mm thick) 5 mm to membrane	Anolyte and catholyte in continuos closed loop mode, 21C
Li_Recovery_Dual_Flow_Cell 20110111	0.2 M Li2S in MF	Glassy carbon plate (1.65"x1.75", 0.5 mm thick) 3 mm to membrane	LiSICON 10B 1.5" Diam., 1 mm thick	1M LiI in TG	Titanium mesh (1.65"x1.75", 0.2 mm thick) 5 mm to membrane	Anolyte and catholyte in continuos closed loop mode, 21C
Li_Recovery_Dual_Flow_Cell 20110208	0.2 M Li2S in MF	Glassy carbon plate (1.65"x1.75", 0.5 mm thick) 3 mm to membrane	LiSICON 10B 1.5" Diam., 1 mm thick	1M LiI in TG	Titanium mesh (1.65"x1.75", 0.2 mm thick) 5 mm to membrane	Anolyte and catholyte in continuos closed loop mode, 50C
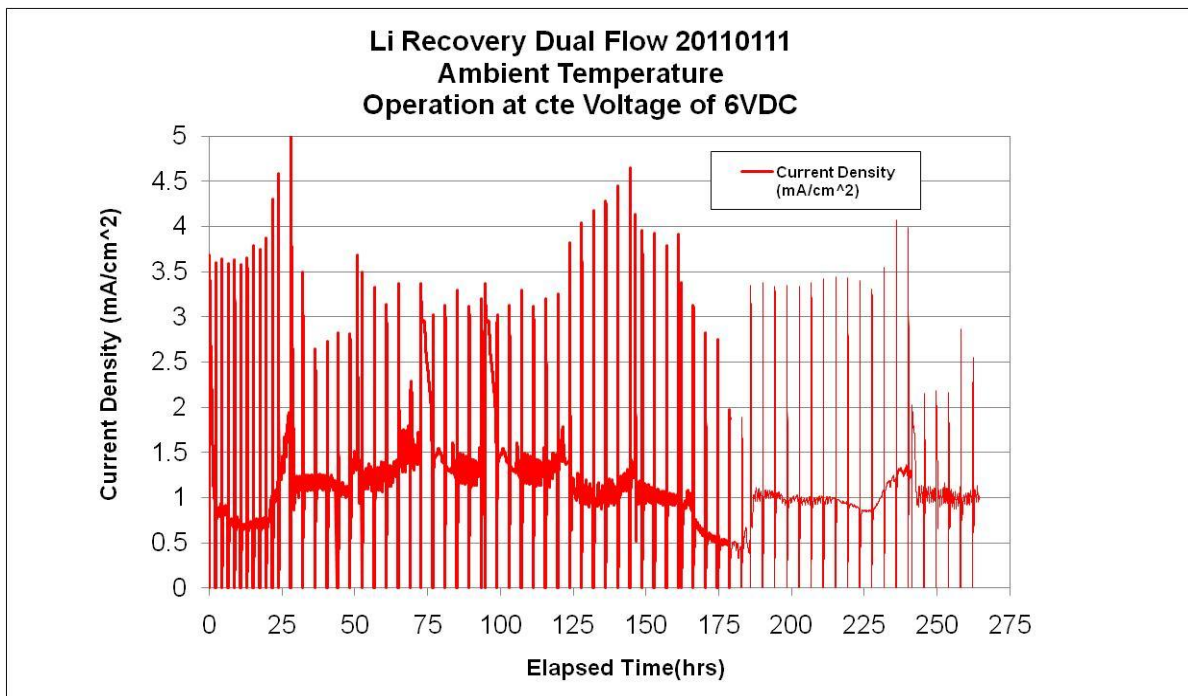
Figure 12: Cell current density vs. elapsed time at 6 VDC constant voltage for *Li Recovery Dual Flow 20110111* cell. Cell was run in closed loop continuous mode at ambient temperature
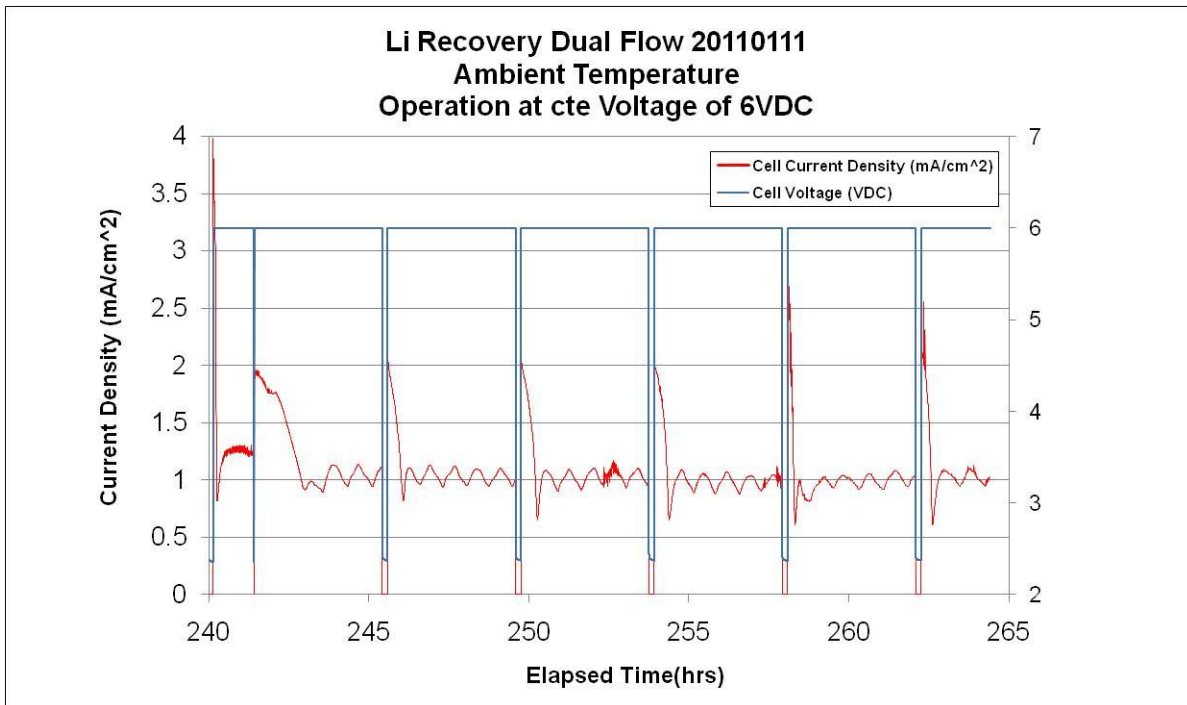
Figure 13: Cell current density and cell voltage vs. elapsed time (from 240 to 260 hours) at 6 VDC constant voltage for *Li Recovery Dual Flow 20110111* cell. Cell was run in closed loop continuous mode at ambient temperature.
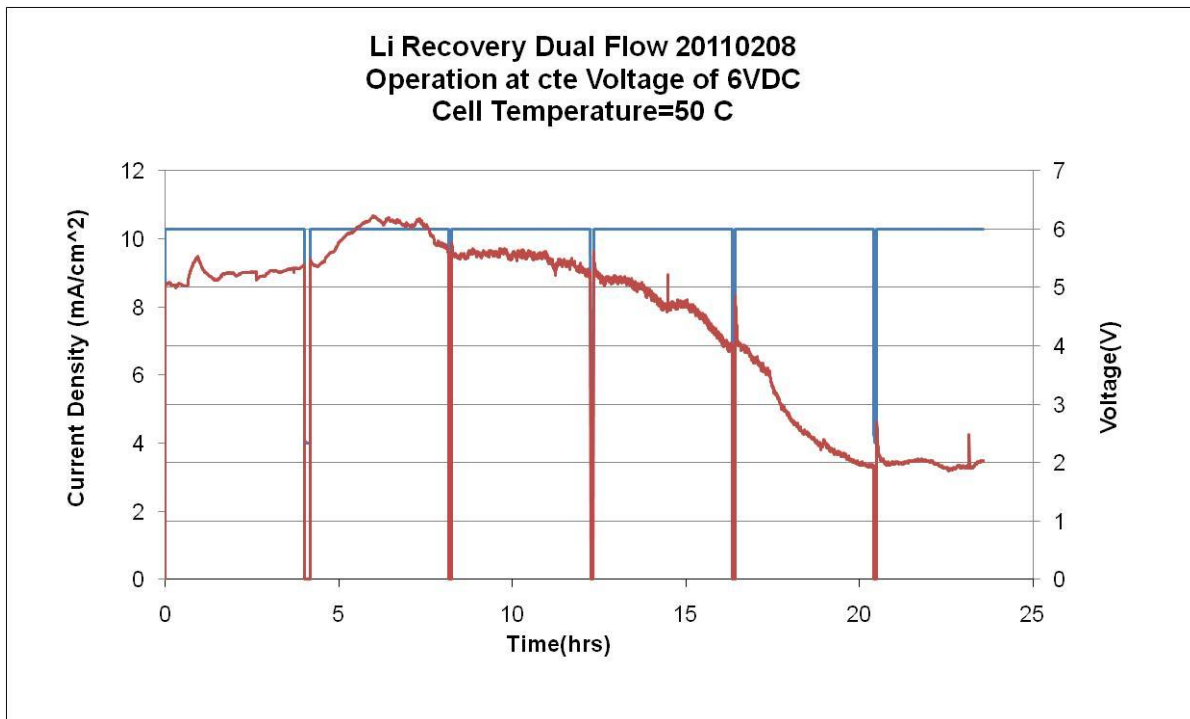
Figure 14: Cell current density and voltage vs. elapsed time at 6 VDC constant voltage for *Li Recovery Dual Flow 20110208* cell. Cell was run in closed loop continuous mode at a temperature of 50°C
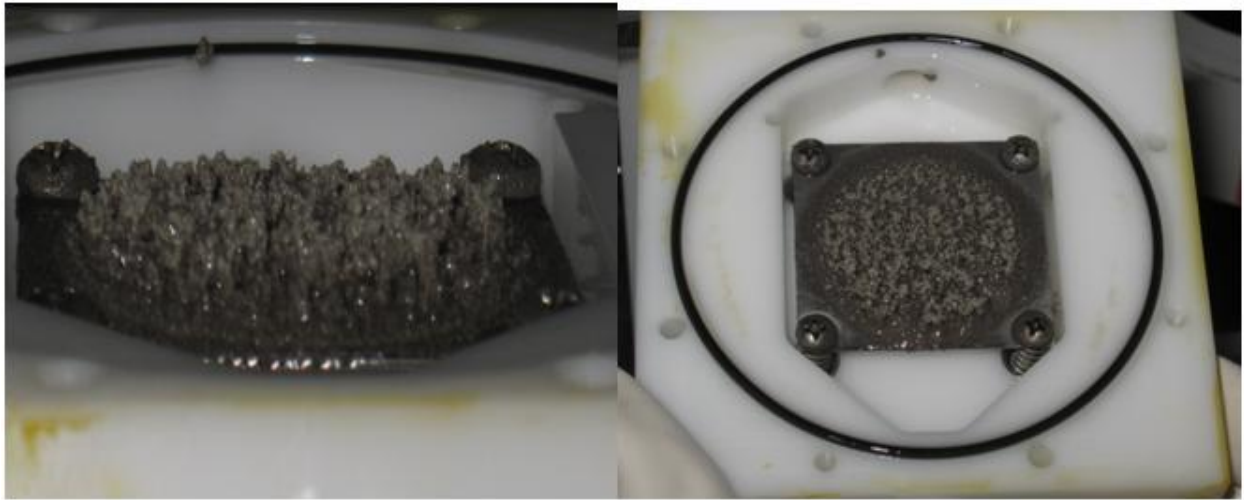
Figure 15: Side [A] and top [B] views of lithium metal deposit on the titanium cathode electrode of *Li Recovery Dual Flow 20110111*
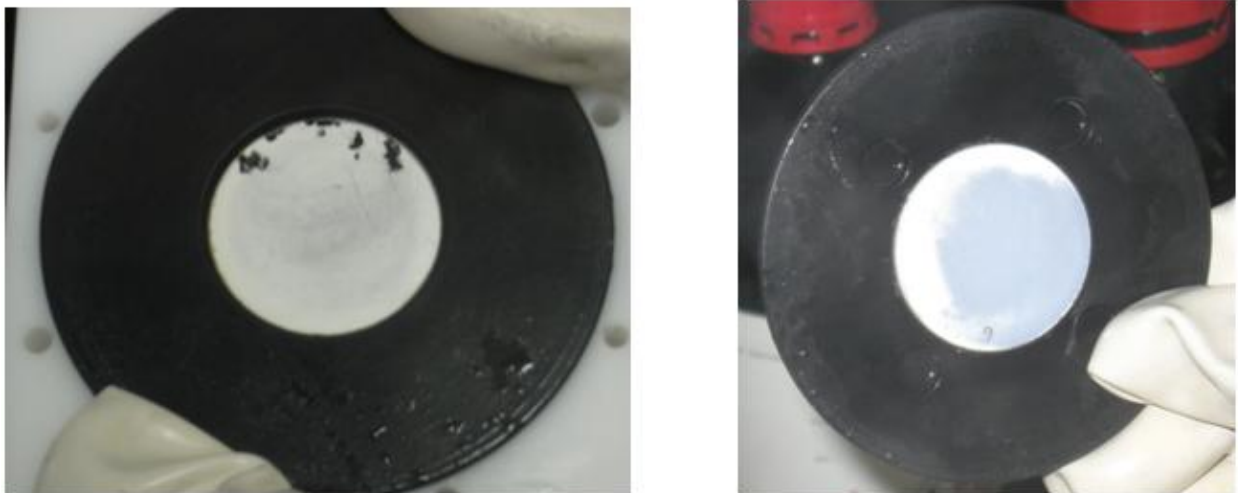
Figure 16: Cathode [A] and anode [B] sides of the LiSICON 10B membrane from *Li Recovery Dual Flow Cell 20110111* **after 28 hours of operation**
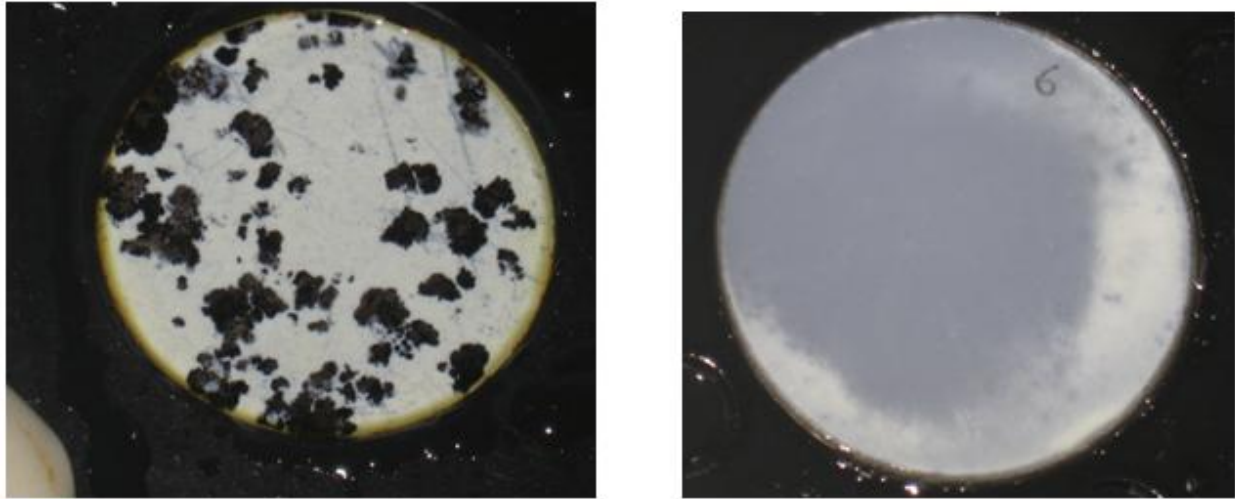
Figure 17: Cathode [A] and anode [B] sides of the LiSICON 10B membrane from *Li Recovery Dual Flow Cell 20110111* at the end of the run

2.5   Task 4.0 – Analysis

2.5.1   Subtask 4.1 – Develop upgrading process model

Ceramatec shall evaluate several process variables in Task 2 which will impact the effectiveness of impurity removal, saturation, coking, and alkali metal utilization. In addition, the shale oil source and initial composition is likely to be a factor. Extent of hydrogen donation gas added and presence of hydrotreating catalyst will affect the extent of upgrading. A preliminary model based on the data from Task 2 will be constructed.

In the last quarterly report mass and energy balances of the upgrading reaction process was presented. This report focuses on the cost estimation part of the shale oil upgradation project. The cost model primarily consists of capital and operating costs for a 25000 BPD capacity oil refinery plant. Three different types of oil feedstocks (Shale Oil 1, Shale Oil 2, and Heavy Oil 1) were considered. The process schematic, which includes all the major pieces of equipment, is shown in Figure 18. The flow rates displayed in the figure correspond to the case with Shale Oil 1.
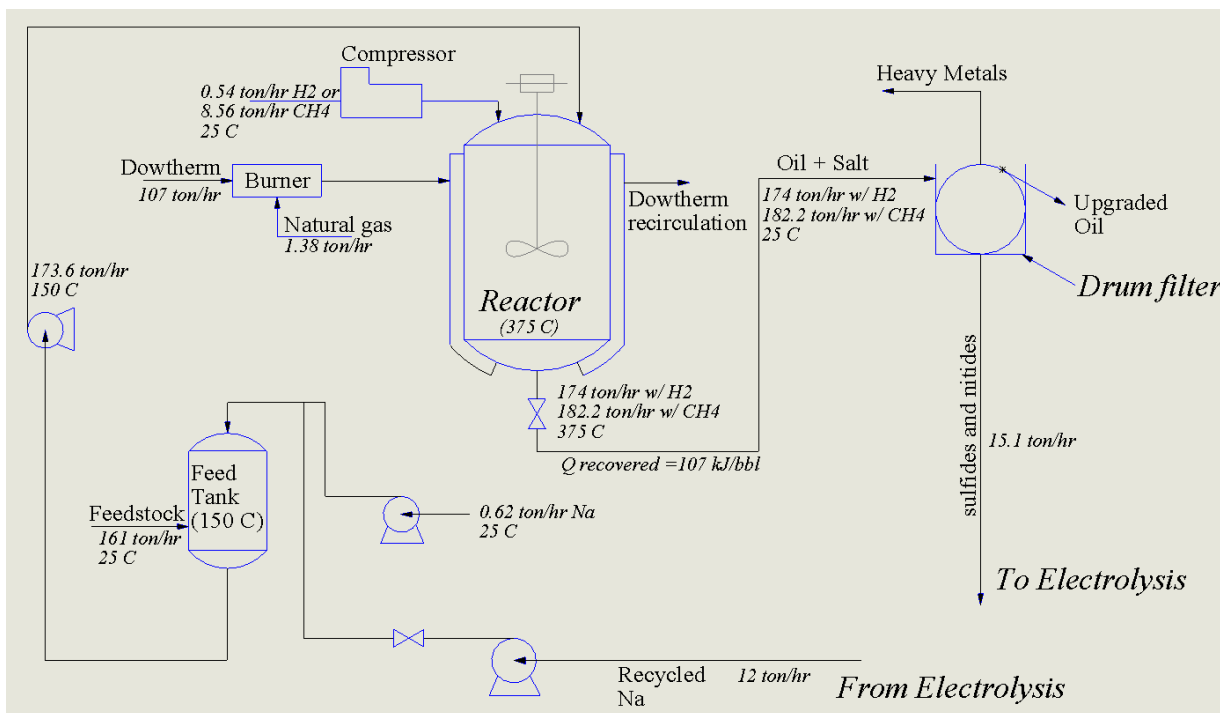
Figure 18: Oil flow diagram showing the key components

2.5.2   Subtask 4.2 – Develop electrolysis process model

Ceramatec shall analyze data from Task 3 and a performance model will be developed. Various factors such as membrane thickness, type of alkali metal, electrode configuration and cell design would be included in the model considerations.

The overall electrolysis process, with all the input and output streams, is sketched in Figure 19. A low sulfur to alkali metal ratio polysulfide (M_2S_x) solution stream and a make-up fresh solvent stream enter the process. Three output streams consisting of a high sulfur to alkali metal polysulfide (M_2S_y) solution, sulfur, and alkali metal (M) leave the process. In the figure, M could be sodium or lithium and the index *y* is greater than *x*. Electrical power to drive the electrolysis reactions, pump the electrolytes, maintain the cell operating temperature, and others is needed.

Since the single largest operating cost of the process is the electric power required for the electrolysis reactions to occur, minimizing the cell voltage should be one main optimization goals. The specifics of the electrolysis process are highly dependent on the alkali metal that needs to be recovered. Figure 20 and Figure 21 show the schematics of two proposed processes to recover sodium and lithium metal, respectively. The anolyte side of the two processes is basically identical. The polysulfide salts (M_2S_x) are transported into the anolyte mixing tank, where they are dissolved into the anolyte solvent and heated up to the cell operating temperature. A recycled stream of the polysulfide (M_2S_y) solution can be returned back to the cell for further sulfur and alkali metal recovery. The low solubility of sulfur in the anolyte solvent will make it to precipitate as it forms in the cell. Therefore, the output stream of the cell will consist of a slurry containing the undissolved sulfur and the dissolved polysulfides. The stream is first cooled and then transported into a sedimentation tank, where the light and the slurry phases are separated. The slurry phase is then washed and the solid sulfur is filtered in a rotary vacuum-drum filter.

The polysulfide solution is then pumped into the separation process (not shown in the schematic), where the polysulfide salts and the solvent are separated. The lithium and sodium processes differ on the catholyte side. While molten sodium is the catholyte in the sodium recovery process, a non-molten organic solvent catholyte is used for lithium recovery. Molten sodium is continuously removed from the cathode chamber at the same rate at which it is being produced. The molten metal is pumped to a molten sodium storage tank from where it is transported to the oil upgrading reactor. During the startup operations, the cell will be primed with molten sodium from the storage tank. Due to the high melting temperature of lithium, an organic solvent based catholyte, with a dissolved supporting electrolyte, is preferred for the separation of lithium. Lithium metal is plated at the cathode electrode, from where it can be removed in continuous or batch operating mode. The catholyte solution is continuously circulated through the cell from a mixing tank, where make-up catholyte solvent can be added as needed. It is advantageous to the process to maintain a high flow rate through the cell to achieve good mixing through the electrode and ceramic membrane interfaces.
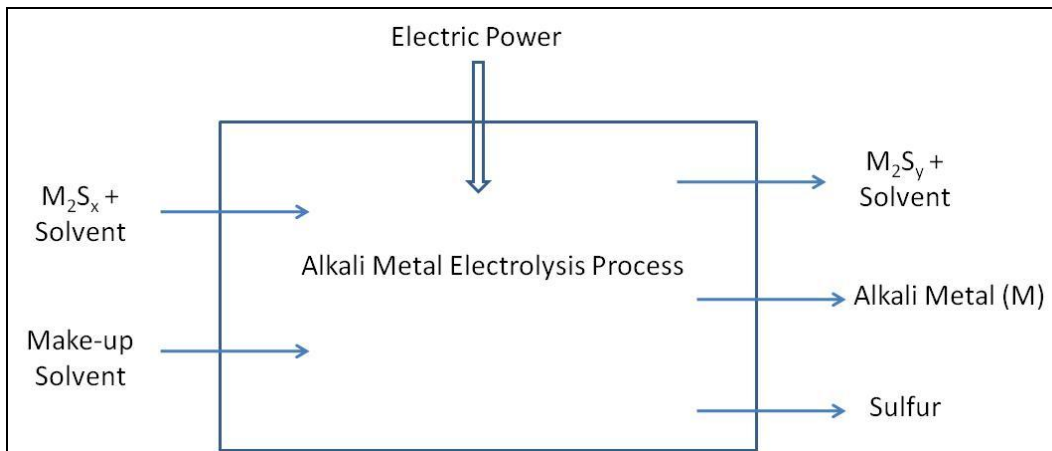
Figure 19: Simplified alkali metal electrolytic recovery process schematic
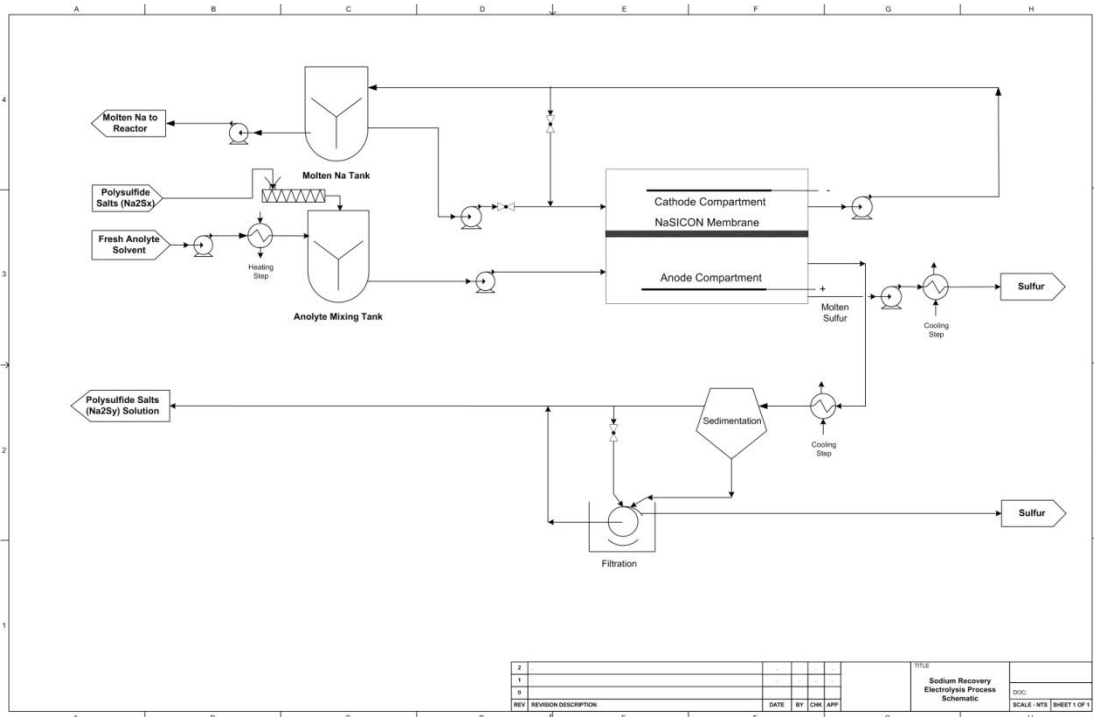
Figure 20: Schematic of the proposed sodium electrolytic recovery process
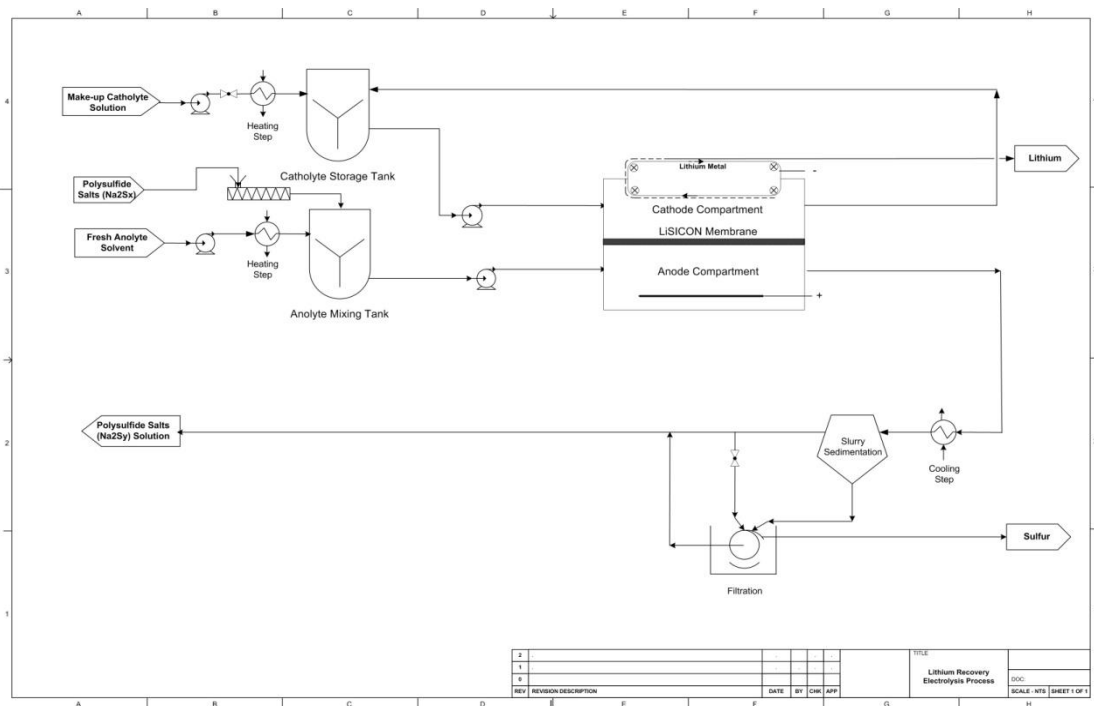
Figure 21: Schematic of the proposed lithium electrolytic recovery process

Overall mass balances have been done for the proposed sodium and lithium recovery processes based on four different types of oil feedstocks to be upgraded. These oils include Red Leaf and OSEC shale oils, a San Joaquin heavy oil and a generic bitumen.

Table 7 lists the API value, specific gravity and the sulfur and nitrogen contents of the oils. A 25,000 barrels per day oil updgrading facility has been adopted as the calculation basis for the material balances. Table 8 and Table 9 show the steady state stream mass flow rates for the sodium and lithium processes, respectively. Below there is a list of the main assumptions used in these calculations:

- No alkali metal or anolyte loses through the process.
- The concentrations of sodium and lithium polysulfide (M_2S_3) in the inlet anolyte stream are equal to 1M.
- All the sulfur and nitrogen originally present in the oil have been converted to alkali polysulfide (M_2S_3) in the upstream reaction and separation processes. Nitrogen is initially converted to an alkali metal nitride and then to ammonia and alkali metal polysulfide. Two and three mols of alkali metal are needed to convert each mol of sulfur and nitrogen, respectively, present in the oil.
- 100% current efficiency or 100% selectivity towards the desired redox reactions.
- All the physical properties of the streams inside the cell have been estimated at 150°C.
- All the elemental sulfur (S_8) formed in the electrolytic cell has been assumed to precipitate. Therefore, there is not elemental sulfur present in the inlet and outlet anolyte streams.
- Assumed Redox reactions:

Cathode Reaction: $2M^+ + 2e^- \rightarrow 2M$

Anode Reaction: $3/2 \ M_2S_3 \rightarrow 2M^+ + ½ \ M_2S_6 + 3/16 \ S_8 + 2e^-$

Overall Reaction: $¾ \ M_2S_3 \rightarrow M + ¼ \ M_2S_6 + 3/32 \ S_8$
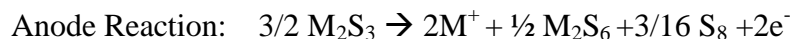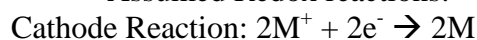
Table 7: Properties and composition of the oils used in the study

Type of oil	Origin	API Value	Specific Gravity	S Content	N Content
				%	%
Shale Oil 1	Red Leaf	35.29	0.848	0.25	1.48
Shale Oil 2	OSEC	35.29	0.840	0.84	0.47
Heavy Oil 1	San Joaquin	10.78	0.995	1.54	0.76
Bitumen		5.4	1.034	4.4	0.6

Table 8: Basic mass balance for the electrolytic sodium recovery process

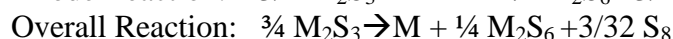| Type of oil	Oil Quantity Processed	Na2S3 Salts Inlet	Fresh Anolyte Solvent	Na2S3 Solution Inlet	Na2S6 Solution Outlet	Na2S6 Salts Outlet	Sulfur as S8	Sodium Metal Recovered
	barrel/day	ton/day	ton/day	ton/day	ton/day	ton/day	ton/day	ton/day
Shale Oil 1	25,000	1196.46	8502.02	9698.49	9170.63	926.67	269.79	258.06
Shale Oil 2	25,000	414.10	2942.59	3356.69	3173.99	320.73	93.38	89.32
Heavy Oil 1	25,000	1091.44	7755.73	8847.17	8365.65	845.33	246.11	235.41
Bitumen	25,000	1765.75	12547.34	14313.09	13534.08	1367.59	398.16	380.85

Table 9: Basic mass balance for the electrolytic lithium recovery process

Type of oil	Oil Quantity Processed	Li2S3 Salts Inlet	Fresh Anolyte Solvent	Na2S3 Solution Inlet	Li2S6 Solution Outlet	Li2S6 Salts Outlet	Sulfur as S8	Lithium Metal Recovered
	barrel/day	ton/day	ton/day	ton/day	ton/day	ton/day	ton/day	ton/day
Shale Oil 1	25,000	926.19	8501.15	9427.34	9079.67	656.40	269.79	77.88
Shale Oil 2	25,000	320.56	2942.28	3262.84	3142.51	227.18	93.38	26.95
Heavy Oil 1	25,000	844.89	7754.93	8599.82	8282.67	598.78	246.11	71.04
Bitumen	25,000	1366.87	12546.06	13912.93	13399.84	968.72	398.16	114.93

The mass flow rate stream of recovered lithium metal is 3.3 times smaller than sodium due to the difference in atomic weights of the two metals. For the same reason, the mass of the lithium polysulfide salts are also smaller than the sodium salts. However when comparing the anolyte flow rates the amounts are very similar. In terms of the different oil feedstocks, obviously the bitumen requires the largest amount of alkali metal since it has the highest S and N content of the four.

Basic energy balances of the processes were also conducted. The following assumptions were followed:
- The cells are maintained in isothermal conditions.
- The fresh anolyte solvent and the polysulfide salts are introduced into the anolyte mixing tank at ambient temperature conditions.
- The electrolyte input and output streams enter and leave the electrolytic cell at the cell's temperature.
- The alkali metal leaves the cell at the cell's temperature.

- The Joule heating generated within the cell during operation is removed and used to pre-heat the incoming anolyte stream. Above a certain cell current density value, the cell's Joule heating exceeds the heat needed to preheat the anolyte stream and therefore extra cooling is required to maintain cell's isothermal conditions. This model assumes that this extra heat is not recovered and it is accounted as a heat loss.
- There are not heat losses within the cell.
- There are no heat loses from the electrolyte solutions in the plumbing from the cell to the storage and mixing tanks.
- The outlet polysulfide and sulfur streams are cooled down in a cooling step prior to entering the sedimentation and filtration steps. This heat is not recovered and it is accounted as a heat loss.

The cell voltage is a critical parameter since it determines the cell operating power. It is most importantly affected by the operating cell current density, cell temperature, electrolyte type, and cell design. Models to estimate the cell voltage for the lithium and sodium recovery processes have been developed. Basically, the total cell voltage (Eq. 1) consists of the sum of the Nernst potential E_{Nernst}, the activation potentials $E_{Activation}$, and the Ohmic potential E_{Ohmic}

$$E_{cell} = E_{Nernst} + E_{Activation} + E_{Ohmic} \qquad \text{[Eq. 1]}$$

E_{Nernst} is a thermodynamic property that depends on the cell temperature and the activities of the reaction species. The Nernst potential is the only component of the total cell potential that is not current density dependent. The Activation potential consists of the sum of the cathodic and the anodic activation potentials. They are related to the kinetics of electron transfer at the cathode and anode electrodes. In general, fast reactions have low activation energies, while slow reactions have high activation energies. The activation potentials can be experimentally determined by fitting the experimental data to the Tafel Equation. The Ohmic potential or voltage drop is equal to the current times the total resistant of the cell. The overall resistance is equal to the sum of all the in-series resistances of the cell (Eq. 2). I is the cell current density.

$$E_{Ohmic} = I * R_{cell} = I * \sum_i R_i^{cell} = I*(R_{catholyte} + R_{membrane} + R_{anolyte} + R_{other}) \qquad \text{[Eq. 2]}$$

The resistances due to catholyte, membrane and anolyte can be estimated from the knowledge of the ionic conductivities (σ_i) of the electrolytes and the membrane material from Equation 3. The ionic conductivities are temperature dependent. In addition, the electrolyte ionic conductivities are a function alkali polysulfide concentration.

$$R_i = (1/\sigma_i)*d_i \qquad \text{[Eq. 3]}$$

In Eq. 3, d_i is the characteristic length scale, which is the distance between the membrane and the electrodes (for the electrolytes contribution) and the thickness for the membrane contribution. Under R_{other}, we have added other contributions to the overall cell resistance such as the current collectors, bus bars, connection wires, etc.

Both $E_{activation}$ and E_{Ohmic} increase with current density and are regarded as energy inefficiencies and they are converted into heat released in the cell.

Figure 22 shows the comparison between the estimated voltages for the sodium and lithium cells. The Nernst potential for the reduction of lithium is 0.326 volts higher than that of sodium. Also, the voltage drop due to the catholyte in the sodium cell (molten sodium) is insignificant as compared to the solvent-based catholyte (Tetraglyme+LiI) in the lithium cell. These two factors explain the higher voltage of the lithium cell versus the sodium cell.
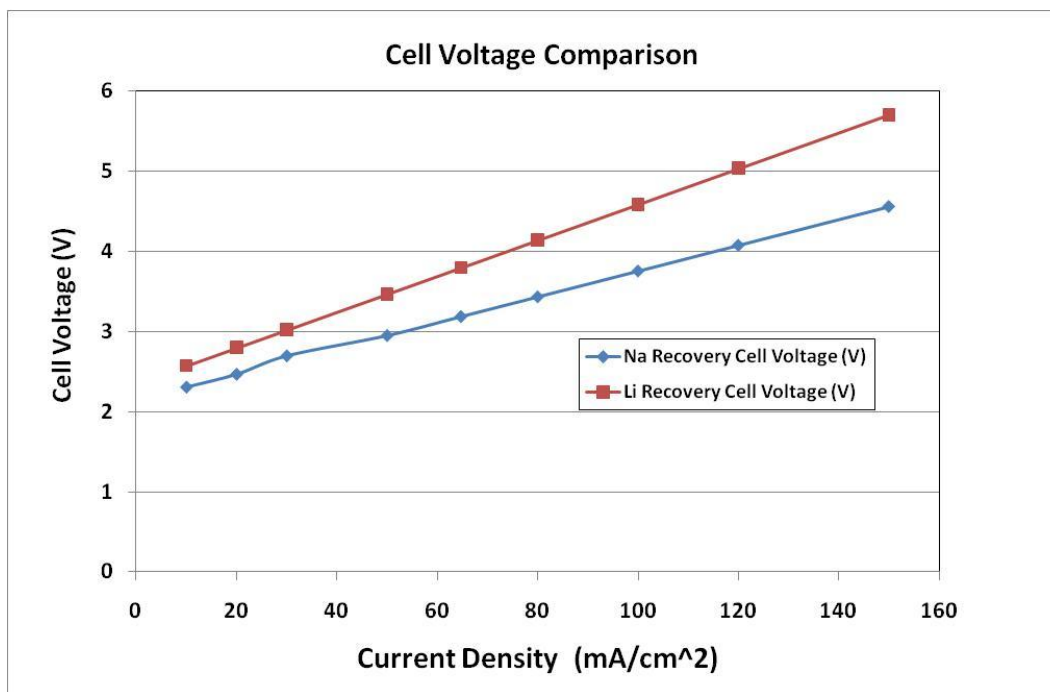
Figure 22: Estimated operating voltages for the sodium and lithium recovery cells at 150ºC with 500 micron thick membranes (NaSICON-GY and LiSICON 10B) with a 3 mm electrode to membrane distance

2.5.3   Subtask 4.3 – Preliminary cost analysis

The Recipient shall incorporate the models from Subtasks 4.1 and 4.2 into a preliminary cost model. Based on the preliminary cost analysis, a selection will be made between sodium and lithium as the most promising alkali metal for further pursuit in Phase 2.

Preliminary cost analysis for reaction step

Key assumptions made for the capital cost estimation are as follows:

- Mechanical efficiencies of rotating equipment, such as the compressor and the reactor agitator were considered to be 85%.
- The reactor is heated up to 375 C using Dowtherm heating oil. The oil is heated against hot flue gas generated from burning natural gas.

- Sizing and costing of the process equipment was done by applying engineering rules of thumb and scaling factors.

Table 10 shows the equipment cost. The major plant capital investments include the reactor vessel, the NG/H2 compressor, and the heating oil. The cost of other equipment, such as feed tank, agitator, and drum filter are included under the name "other equipments.

Table 10: Total equipment cost

Type of Oil	Reactor	Compressor	Heating Oil	Other Equipments	Total equipment cost
	(MM$)	(MM$)	(MM$)	(MM$)	(MM$)
Shale Oil 1	2.59	2.5	0.21	0.442	5.472
Shale Oil 2	2.59	2.5	0.21	0.442	5.472
Heavy Oil 1	2.59	2.5	0.21	0.442	5.472

Capital costs for different oils remain same because the difference in their stoichiometric values is not big enough to affect the sizes of the processing equipment. Costs of Installed piping & fitting, equipment installation, instrumentation & control, and facilities are assumed to be 15, 30, 13, and 40 percent respectively. Assuming a 15 year plant life expectancy of continuous operation, the total capital cost per barrel of oil is reported in the last column of Table 11.

Table 11: Total capital cost

Type of Oil	Total equipment cost	Installed Piping & Fittings	Equipment installation	Instrumentation and controls	Facilities	Total capital cost	
	(MM$)	(MM$)	(MM$)	(MM$)	(MM$)	(MM$)	($/bbl oil)
Shale Oil 1	5.472	0.861	1.723	0.746	2.297	11.369	0.083
Shale Oil 2	5.472	0.861	1.723	0.746	2.297	11.369	0.083
Heavy Oil 1	5.472	0.861	1.723	0.746	2.297	11.369	0.083

The operating costs are sensitive to the required amounts of hydrogen/methane and sodium needed to remove all the sulfur and nitrogen present in the oil. Therefore, they vary depending on the type of oil upgraded. Major operating costs correspond to the raw materials: methane/hydrogen and 5% sodium losses. Other costs include the cost of natural gas required to heat Dowtherm and the cost of power needed to operate the mechanical equipment. In the estimation, it is assumed that up to 75 % of the latent heat of the reactor products is recovered to pre-heat the incoming reactants. Therefore, only 25% of the energy needed to preheat the oil needs to be generated from the natural gas. Labor cost is assumed as 15% of the sum of all operating costs. Table 12 and Table 13 show the operating cost of the plant for the cases of hydrogen and methane treating respectively.

Table 12: Total operating cost with hydrogen treating

Reaction Step Operating Costs using Hydrogen for 25,000 barrels/day Plant Capacity						
Type of Oil	Hydrogen for Rx.	Sodium Loss	Rx. Heating	Power	Labor	Total
	$/bbl oil	$/bbl oil	$/bbl oil	$/bbl oil	$/bbl oil	$/bbl oil
Shale Oil 1	1.040	1.180	0.100	0.050	0.356	2.726
Shale Oil 2	0.480	0.540	0.100	0.050	0.176	1.346
Heavy Oil 1	0.800	0.920	0.100	0.050	0.281	2.151

Here we assume $2/kg for hydrogen and $3.84/MMSCF methane.

Table 13: Total operating cost with methane treating

Reaction step operating cost with methane treating						
Type of Oil	Methane for Rx	Sodium Loss	Rx. Heating	Power	Labor	Total
	($/bbl oil)	($/bbl oil)	($/bbl oil)	($/bbl oil)	($/bbl oil)	($/bbl oil)
Shale Oil 1	1.63	1.18	0.1	0.05	0.444	3.404
Shale Oil 2	0.75	0.54	0.1	0.05	0.216	1.656
Heavy Oil 1	1.27	0.92	0.1	0.05	0.351	2.691

Preliminary cost analysis for the electrolysis process

Process Operating Costs

It should be recognized that one of the most important operating parameters of the electrolysis process is the cell current density. For a given constant alkali metal recovery capacity, the higher the current density, the smaller the area of the membrane needed to achieve it. At the same time, a higher current density also implies a higher voltage drop through the cell and therefore higher electrical operating costs. As a result, there is an optimum current density that minimizes the total process cost when the cost of electrical power and the cost of the membranes are accounted. Figure 23 and Figure 24 show that these optimums are equal to 65 mA/cm^2 and 25 mA/cm^2 for the sodium and lithium recovery processes, respectively. In the calculations, it has been assumed that the costs of fabrication of the NaSICON-GY and LiSICON 10B membranes are the same. It has also been assumed that the average expected life of the membranes is 18 months. An electricity cost of 6.59 cents per kw-h has been used in the calculation of the electrolysis cost. At the optimum current density value, the recovery cost of lithium is 4.3 times more expensive than sodium. This is entirely due the higher voltage of the lithium cell as compared to sodium. Given the huge voltage drop disadvantage of the lithium cells, it is clear that from the electrolysis cost point of view, sodium is the preferred alkali metal. As a result, the operating and capital analysis will be done only on the sodium recovery process.

Figure 23: Electrical power and membrane costs as a function of current density, showing the optimum current density according to minimum total cost for the electrolytic sodium recovery process
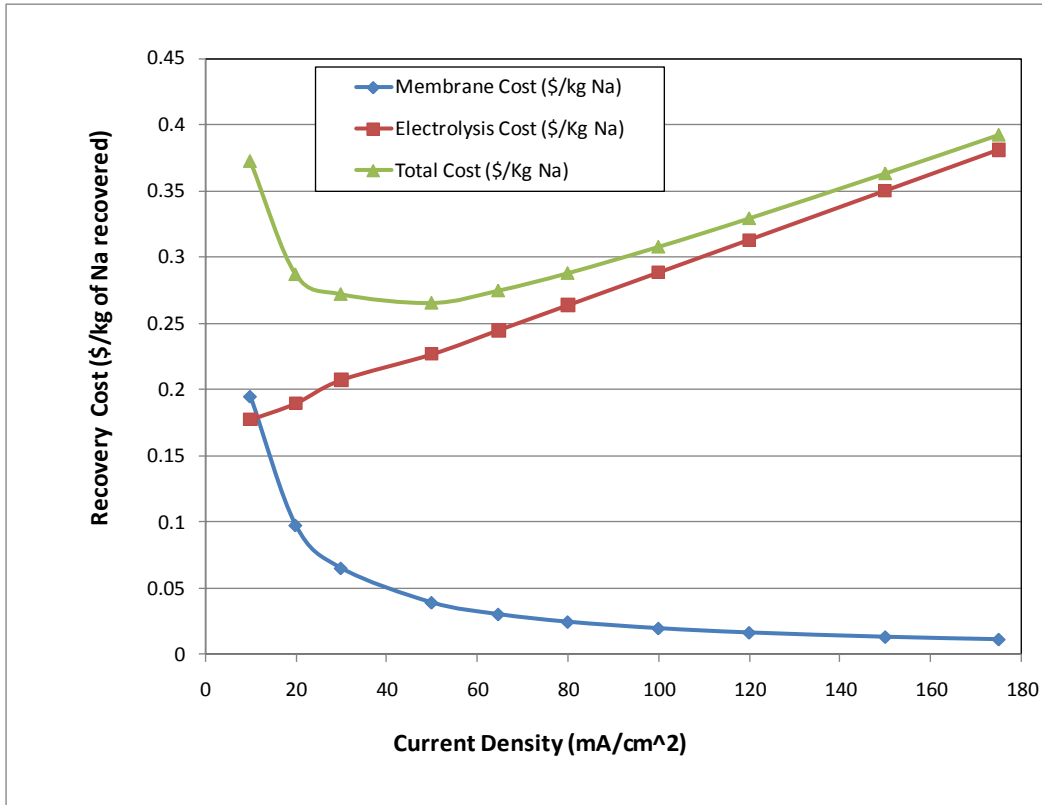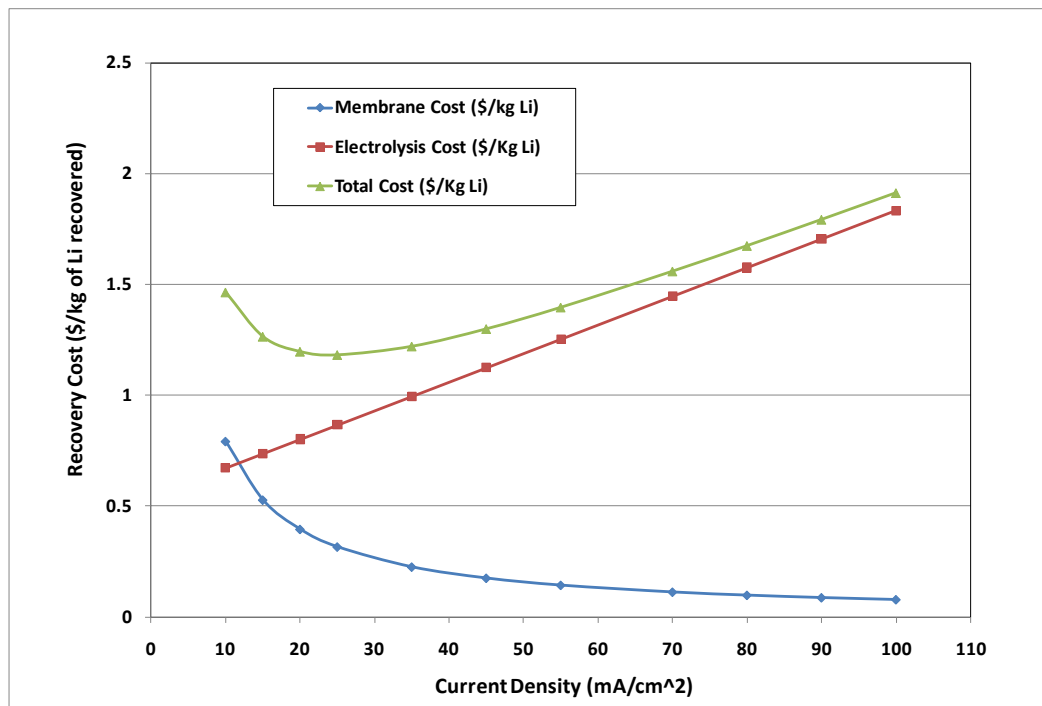

Figure 24: Electrical power and membrane costs as a function of current density, showing the optimum current density according to minimum total cost for the electrolytic lithium recovery process

To estimate the process operating costs, we have identified and focused on the largest cost contributors. These include electrical power, raw material loses, membrane replacement, and labor costs. The electrolysis electrical power costs have been subdivided into cell and non-cell costs. The non-cell items include the electrical costs associated with preheating the anolyte inlet stream to cell temperature conditions, electrolyte and alkali metal pumping, and electrolyte and polysulfide salts mixing in the anolyte stirred tank. We have assumed that the expected life of the ion conductive membranes (e.g. tubes) in the cells is 18 months. The membrane replacement includes the raw materials and fabrication costs, but not the removal of the old and installation of the new membranes. In the raw material loses group we have included the loss of anolyte solvent (e.g. Methylformamide) at a rate of 20% loss per year based on the total anolyte inventory. Labor costs have been calculated as a 15% flat rate of the total operating costs. Table 14 shows the contribution from each of the categories and the total operating costs for the sodium recovery process for the four different types of oil analyzed. We have not included other costs that might quantitatively contribute to the overall costs such as non-membrane maintenance and repairs, general plant utilities, equipment depreciation, taxes, etc. Finally in the cost calculation, the cells are operated at the optimum current density and temperature conditions.

These cost estimates were conducted based on 25,000 barrels of oil per day upgrading plant. However, the operating costs in terms of dollars per barrel of oil are fairly independent on plant capacity due to the linear scaling of the cell electrical power needs with capacity. Figure 25 displays the percent contribution of each of the categories to the total operating costs for Oil Shale #1. Not surprisingly, the cost of electrical power for the electrolysis is the main contributor with 72.6% of the total plant operating costs. Then, it is followed by the labor costs (15%) and by the cost of membrane replacement (8.9%). The cost difference between the different types of oils is due to their different S and N compositions (Table 1).

Table 14: Operating costs (in dollars per barrel of oil) for a sodium recovery electrolysis process, where the cells are operated at the current density and temperature optimum conditions

| Operating Costs at Optimum Current Density=65 mA/cm^2 and Cell Temperature=150°C						
Type of Oil	Cell Power	Non-Cell Power	Raw Materials Losses	Membrane Replacement	Labor	Total
	$/bbl oil	$/bbl oil	$/bbl oil	$/bbl oil	$/bbl oil	$/bbl oil
Shale Oil 1	2.528	0.092	0.029	0.311	0.522	3.482
Shale Oil 2	1.152	0.042	0.016	0.142	0.239	1.591
Heavy Oil 1	2.306	0.084	0.027	0.284	0.477	3.177
Bitumen	3.731	0.134	0.040	0.459	0.770	5.135
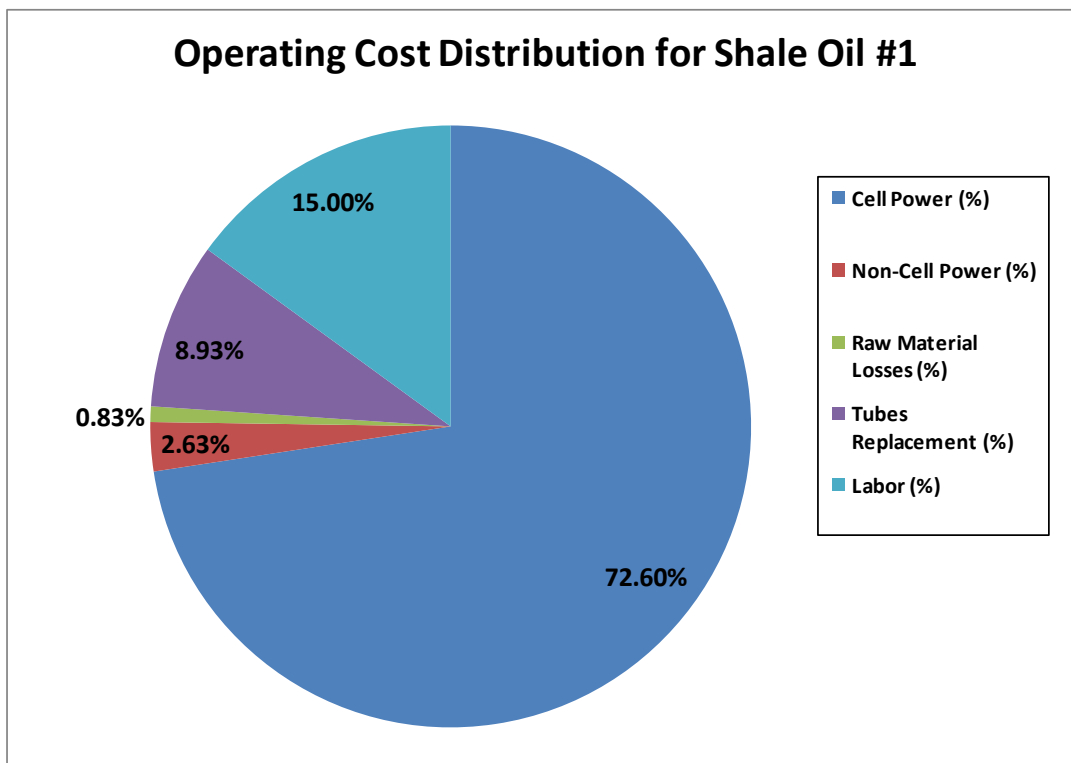
Figure 25: Sodium recovery operating costs distribution for Shale Oil #1

Capital Estimation Costs

The estimation of the capital costs for an electrolytic sodium recovery plant operating at the optimum conditions has been conducted. This estimation covered the cost of the main pieces of equipment, raw materials, equipment installation, installed piping and fittings, instrumentation and controls, basic plant facilities, and the cost of electrical installations. Indirect costs such as engineering and supervision, construction expenses, contractor fees, or contingencies were not considered at this time. Equipment sizing was based on a plant with a capacity of 25,000 barrels of oil per day. Costing of standard pieces equipment such storage and mixing tanks, heat exchangers, filters, pumps, and others was done based on general engineering rules of thumb and order of magnitude scaling.

The electrolysis cells were priced based on the cost of their materials of construction after a basic design was proposed. Raw materials included fresh anolyte solvent and enough sodium to prime the electrolysis cells. A reliable bulk market price of sodium could not be obtained at this time, so a price of $20 per kilo has been assumed for the analysis. The costs of equipment installation, instrumentation & controls, installed piping & fittings, electrical installations, and service facilities were calculated as percentages of the total capital of purchased equipment. The percentages used are approximations based on ordinary chemical processing plants. Table 15 shows the total equipments cost for sodium recovery process and

Table 16 capital cost distribution and the total cost for the four different type of oils considered. The column showing the total cost in terms of dollars per barrel of oil reflects the total

capital investment of the plant divided by an expected plant life of 15 years. Figure 26 displays the capital cost distribution among the different categories as a percent of the total cost for Shale Oil #1.

Not surprisingly, the two priciest pieces of equipment in the plant are the electrolysis cells and electrical transformers-rectifiers. It should be kept in mind that this cost estimation is very preliminary and a large is error (>50%) is expected.

Table 15: Total equipment cost for electrolytic sodium recovery process

Type of Oil	NaSI-CON Tubes	Electro-lysis Cells	Rectifi-ers	Other Equip-ment	Installed Piping & Fittings	Equip-ment Installa-tion	Total equipment cost
	Million $	Million $	Million $	Million $	Million $	Million $	Million $
Shale Oil 1	4.2	7.06	6.8	0.838	2.835	5.67	21.733
Shale Oil 2	1.91	3.32	3.4	0.808	1.409	2.82	10.847
Heavy Oil 1	3.83	6.46	6.8	0.834	2.688	5.38	20.612
Bitu-men	6.2	10.31	10.2	0.856	4.139	8.28	31.705

Table 16: Capital costs (in millions of dollars) for the electrolytic sodium recovery portion of 25,000 barrels per day oil upgrading facility

| Type of Oil	Total equipment cost	Raw Mate-rials	Instrumen-tation & Controls	Electrical Installa-tions	Service Facili-ties	Total Capital In-vestment	
		Million $	Million $	Million $	Million $	Million $	$/barrel oil
Shale Oil 1	21.733	2.51	2.46	2.83	7.56	42.77	0.313
Shale Oil 2	10.847	1.28	1.22	1.41	3.76	21.29	0.156
Heavy Oil 1	20.612	2.31	2.33	2.69	7.17	40.49	0.296
Bitu-men	31.705	3.58	3.59	4.14	11.04	62.36	0.456
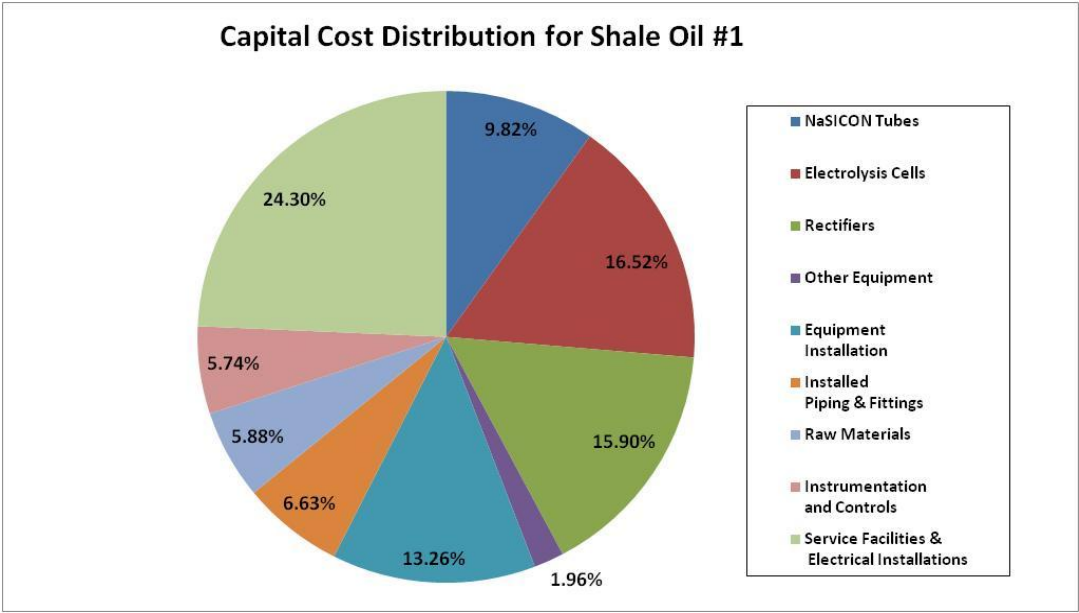
Figure 26: Sodium recovery capital costs distribution for Shale Oil #1

2.5.4   Case study comparison for Heavy Oil upgrading using sodium and comparing hydrogen and methane:

Table 17: Summary of results for hydrogen and methane comparison

	Heavy Oil with H_2 & Na			Heavy Oil with CH_4 & Na		
	In	Out	Convers.	In	Out	Convers.
S/C	1.80%	0.02%	99%	1.80%	0.03%	98%
N/C	0.89%	0.15%	83%	0.89%	0.12%	87%
Fe ppm	218.0	0	100%	218	2.39	99%
V ppm	197.0	0	100%	197	1.31	99%
Ni ppm	331.4	0	100%	331.4	0.85	100%
TAN	4.2	0	100%			
API Gravity	10.78	26.2		10.78	27.21	
g/cc	0.99	0.90		0.99	0.89	
Estimated mass per 100g	100	98.0		100	99.8	
Estimate bbl / bbl	1	1.09		1	1.11	
Capital reactor $/bbl		$ 0.08			$ 0.08	
Capital electrolysis $/bbl		$ 0.34			$ 0.34	
Total capital $/bbl		$ 0.42			$ 0.42	
Operating reactor $/bbl		$ 2.15			$ 2.69	
Operating electrol. $/bbl		$ 3.18			$ 3.18	
Total operating $/bbl		$ 5.33			$ 5.87	
Total costs $/bbl		$ 5.75			$ 6.29	
Credit vol. increase $/bbl		$ 6.86			$ 9.04	
Net upgrading cost		$ (1.11)			$ (2.75)	
Credit for metals $/bbl		$ 6.41			$ 6.37	
Net upgrading cost		$ (7.53)			$ (9.12)	

Table 17 above shows the upgrading process is very effective for both hydrogen and methane in terms of sulfur, nitrogen, heavy metals removal, and increase in API gravity. In the table, the operating costs were assuming $2/kg and methane $3.84/MMSCF, Power $0.0659/kWH. $80 per barrel value of upgraded oil, $100/lb recovered V, $10/lb recovered Ni , and 80% recovery of heavy metals. From the table the total costs to upgrade are about $0.5 per bbl less of hydrogen is used instead of methane. But since the final volume of oil is greater if methane is used, the increase in oil volume after upgrading is worth $2.18 per barrel more when methane is used than when hydrogen is used, thus taking the volume increase in to account, upgrading with methane is more cost effective. If we assume 80% of the vanadium and nickel are recovered, the net upgrading cost is ($9.12) (negative) in the case of methane and ($7.53) for hydrogen. Thus both upgrading processes look promising from a cost perspective not including the further "uplift" resulting in removal of sulfur, nitrogen, and metals.

2.6   Task 5.0 – Reporting

The 6th quarterly report is presently submitted

3. CONCLUSION

Our conclusion at this point is that high levels of both sulfur and nitrogen can be removed from shale oil or heavy oil with the process tested. Nitrogen removal has been less successful with Shale Oil 2 which of the three oils was the least controlled prior to receipt in terms of storage in air and subject to ambient thermal cycles. Both methane and hydrogen are effective in removal of sulfur, nitrogen, heavy metals, and increasing API gravity.

4. COST STATUS

The monthly costs of the 6th quarter are shown in Table 18, along with the projected costs stated in the Project Management Plan.

Table 18: Project costing profile for the 6th Quarter

	Jan-11		Feb-11		Mar-11		Q6	
	Projected	Actual	Projected	Actual	Projected	Actual	Projected	Actual
Direct Labor		25,511.93		19,790.29		25,991.27		71,293.49
Benefits 32%		8,163.82		6,332.89		8,317.21		22,813.92
Overhead 41%		10,459.89		8,114.02		10,656.42		29,230.33
Total Burdened Labor		44,135.64		34,237.20		44,964.90		123,337.74
Direct Materials / Spec Test		31,202.93		29,258.96		38,574.26		99,036.15
Equipment								-
Travel						-		-
Subtotal		75,338.57		63,496.16		83,539.16		222,373.89
G&A 29%		21,848.19		18,413.89		24,226.36		64,488.44
Total monthly	67,115.12	97,186.76	60,237.08	81,910.05	70,063.18	107,765.52	197,415.39	286,862.33

Our costs in the 6th quarter were greater than the projection because there was a lag in ordering equipment early in the project that carried through. Overall the project is ahead of planned spending by approximately 1% over the first 18 months.

Figure 27 shows a plot of the total monthly costs and the initially projected costs versus time and Figure 28 shows the cumulative monthly costs versus time. Also shown in Figure 28 is the fraction of actual over planned cumulative expenses.
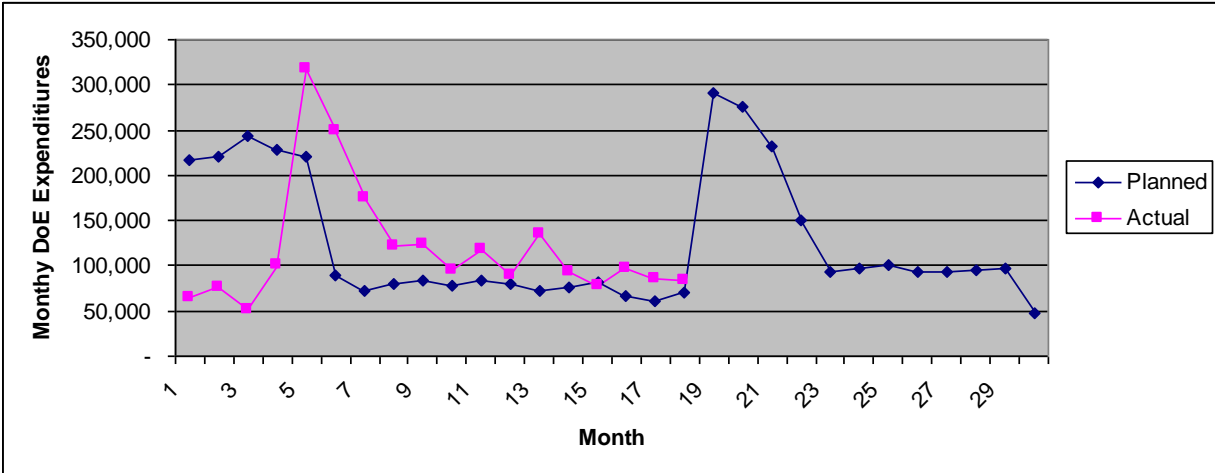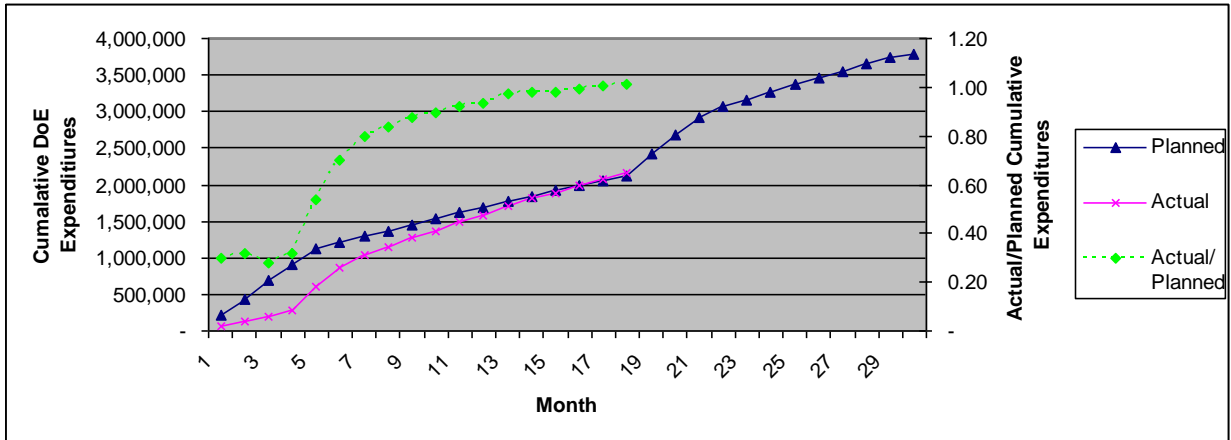
Figure 27: Projected and actual monthly costs over time

Figure 28: Projected and actual cumulative costs over time

5. MILESTONE STATUS

Table 19: Milestone log for 6ʳᵈ Quarter

Mi-les-tone No.	Task / Sub-task	Project Milestone Description	Planned Start Date:	Planned End Date:	Actual Start Date:	Actual End Date:	Comments
1	1	Updated PMP	9/29/09	10/29/09	9/29/09	10/26/09	
2	2.1	Analytic capability established	9/29/09	3/1/10	9/29/09	3/23/10	Analytical capability has been established as stated in the PMP. Operators have been trained on GC. ICP and CHNS are operational
3	2.2	Complete upgrading exp. Setup	9/29/09	3/29/09	9/29/09	3/26/10	Upgrading set-up has been completed including HAZOP and pre-start up safety review. The reactor set up has been ready to be operational as of Friday, March 26, 2010.
4	2.3	Complete process runs	3/30/10	1/3/11	3/26/10	3/31/11	Process runs underway
5	3.1.1	Complete membranes for Phase 1	9/29/09	7/5/10	9/29/09	9/20/10	Membrane fabrication has exceeded demand for fabrication. Mechanical characterization was complete on September 20, 2010.
6	3.3	Cells ready for operation	4/13/10	2/28/11	4/13/10	3/31/11	Cells were ready for operation on time. Initial cells testing began running 4/26/10 when sufficient sodium polysulfide was synthesized.
7	4.3	Preliminary cost model complete	2/8/11	3/14/11	1/4/11	3/18/11	A preliminary cost model was completed and reviewed internally. Adjustments were recommended by the reviewers and additional cases suggested for updated cost models.

6. ACCOMPLISHMENTS

- Electrolysis of sodium sulfide at temperatures of molten sodium have begun and are showing very encouraging results.
- Reactor tests with methane have continued with encouraging results
- Process models of both the reactor and electrolysis processes have begun which will lead to the preliminary cost model.

7. PROBLEMS OR DELAYS

Our Perkin Elmer CHNS analyzer has been unsatisfactory. We have ordered a LECO analyzer as a replacement. In the meantime samples have been sent to an outside lab for analysis.

8. PRODUCTS

No products to report at this time.

9. LIST OF APPENDICES

None

National Energy Technology Laboratory

626 Cochrans Mill Road
P.O. Box 10940
Pittsburgh, PA 15236-0940

3610 Collins Ferry Road
P.O. Box 880
Morgantown, WV 26507-0880

13131 Dairy Ashford, Suite 225
Sugar Land, TX 77478

1450 Queen Avenue SW
Albany, OR 97321-2198

2175 University Ave. South
Suite 201
Fairbanks, AK 99709

Visit the NETL website at:
www.netl.doe.gov

Customer Service:
1-800-553-7681